University of Glasgow

Blockley, S. P.E., Edwards, K. J., Schofield, J. E., Pyne-O'Donnell, S. D.F., Jensen, B. J.L., Matthews, I. P., Cook, G. T., Wallace, K. L., and Froese, D. (2015) First evidence of cryptotephra in palaeoenvironmental records associated with Norse occupation sites in Greenland.*Quaternary Geochronology*, 27, pp. 145-157.

Copyright © 2015 Elsevier B.V.

A copy can be downloaded for personal non-commercial research or study, without prior permission or charge

Content must not be changed in any way or reproduced in any format or medium without the formal permission of the copyright holder(s)

http://eprints.gla.ac.uk/104464/

Deposited on: 27 March 2015

Enlighten – Research publications by members of the University of Glasgow
http://eprints.gla.ac.uk

Accepted Manuscript

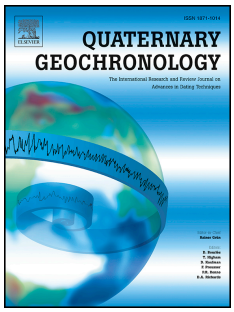

First evidence of cryptotephra in palaeoenvironmental records associated with Norse occupation sites in Greenland

Simon P.E. Blockley, Kevin J. Edwards, J. Edward Schofield, Sean D.F. Pyne-O'Donnell, Britta J.L. Jensen, Ian P. Matthews, Gordon T. Cook, Kristi L. Wallace, Duane Froese

PII: S1871-1014(15)00036-9

DOI: 10.1016/j.quageo.2015.02.023

Reference: QUAGEO 649

To appear in: *Quaternary Geochronology*

Received Date: 26 March 2014

Revised Date: 13 February 2015

Accepted Date: 24 February 2015

Please cite this article as: Blockley, S.P.E., Edwards, K.J., Schofield, J.E., Pyne-O'Donnell, S.D.F., Jensen, B.J.L., Matthews, I.P., Cook, G.T., Wallace, K.L., Froese, D., First evidence of cryptotephra in palaeoenvironmental records associated with Norse occupation sites in Greenland, *Quaternary Geochronology* (2015), doi: 10.1016/j.quageo.2015.02.023.

This is a PDF file of an unedited manuscript that has been accepted for publication. As a service to our customers we are providing this early version of the manuscript. The manuscript will undergo copyediting, typesetting, and review of the resulting proof before it is published in its final form. Please note that during the production process errors may be discovered which could affect the content, and all legal disclaimers that apply to the journal pertain.

ACCEPTED MANUSCRIPT

Science Highlights

We examine the chronologies and palynological record from Iconic Norse Viking sites in Greenland

This is the first identification of distal tephra in Greenland Viking sites#

We demonstrate the potential for tephra to add new chronological underpinning to the timing of Norse occupation of Greenland

We show that tephra are travelling to Greenland Viking sites from North America

ACCEPTED MANUSCRIPT

ACCEPTED MANUSCRIPT

First evidence of cryptotephra in palaeoenvironmental records associated with Norse occupation sites in Greenland

Simon P.E. Blockley [a,*], Kevin J. Edwards [b,c], J. Edward Schofield [b], Sean D.F. Pyne-O'Donnell [d], Britta J.L. Jensen [d,e], Ian P. Matthews [a], Gordon T. Cook [f], Kristi L. Wallace [g] and Duane Froese [e]

[a] Department of Geography, Royal Holloway University of London, Egham, Surrey, TW20 0EX, UK

[b] Department of Geography & Environment, School of Geosciences, University of Aberdeen, Elphinstone Road, Aberdeen, AB24 3UF, UK

[c] Department of Archaeology, School of Geosciences, University of Aberdeen, Elphinstone Road, Aberdeen, AB24 3UF, UK

[d] School of Geography, Archaeology and Palaeoecology, Queen's University Belfast, Belfast, BT7 1NN, UK

[e] Department of Earth and Atmospheric Sciences, University of Alberta, Edmonton, AB T6G 2E3, Canada

[f] SUERC Radiocarbon Dating Laboratory, Scottish Universities Environmental Research Centre, Scottish Enterprise Technology Park, East Kilbride G75 0QF, UK

[g] U.S. Geological Survey, Alaska Science Centre, 4210 University Dr., Anchorage, AK 99508-4626

* Corresponding Author Dr Simon Blockley, Department of Geography, Royal Holloway University of London, Egham, Surrey, TW20 0EX, UK simon.blockley@rhul.ac.uk Tel. +441784443045

ABSTRACT

The Norse/Viking occupation of Greenland is part of a dispersal of communities across the North Atlantic coincident with the supposed Medieval Warm Period of the late 1st millennium AD. The abandonment of the Greenland settlements has been linked to climatic deterioration in the Little Ice Age as well as other possible explanations. There are significant dating uncertainties over the time of European abandonment of Greenland and the potential influence of climatic deterioration. Dating issues largely revolve around radiocarbon chronologies for Norse settlements and associated mire sequences close to settlement sites. Here we show the potential for moving this situation forward by a combination of palynological, radiocarbon and cryptotephra analyses of environmental records close to three 'iconic' Norse sites in the former Eastern Settlement of Greenland – Herjolfsnes, Hvalsey and

ACCEPTED MANUSCRIPT

Garðar (the modern Igaliku). While much work remains to be undertaken, our results show that palynological evidence can provide a useful marker for both the onset and end of Norse occupation in the region, while the radiocarbon chronologies for these sequences remain difficult. Significantly, we here demonstrate the potential for cryptotephra to become a useful tool in resolving the chronology of Norse occupation, when coupled with palynology. For the first time, we show that cryptotephra are present within palaeoenvironmental sequences located within or close to Norse settlement ruin-groups, with tephra horizons detected at all three sites. While shard concentrations were small at Herjolfsnes, concentrations sufficient for geochemical analyses were detected at Igaliku and Hvalsey. WDS-EPMA analyses of these tephra indicate that, unlike the predominantly Icelandic tephra sources reported in the Greenland ice core records, the tephra associated with the Norse sites correlate more closely with volcanic centres in the Aleutians and Cascades. Recent investigations of cryptotephra dispersal from North American centres, along with our new findings, point to the potential for cryptotephra to facilitate hypothesis testing, providing a key chronological tool for refining the timing of Norse activities in Greenland (e.g. abandonment) and of environmental contexts and drivers (e.g. climate forcing).

Keywords: Greenland, Norse, tephra, palynology, radiocarbon

1. Introduction

The Norse/Viking occupation of Greenland was part of the spread of human communities across a largely uninhabited North Atlantic region. The colonizers came from Scandinavian homelands and, in part, from the British Isles, at times coincident with the supposed Medieval Warm Period of the late 1st millennium AD (Ingstad, 1966; Fitzhugh and Ward, 2000; Dugmore et al., 2005). Although the initial date of settlement (*landnám*; 'land-taking') in Greenland is historically documented and accepted at AD 985 (Krogh, 1967), the date of abandonment by the Norse is less secure, as indeed are the reasons for the ultimate demise of European colonies. Climate is often implicated in this process – especially the Little Ice Age (Grove, 1988) – but many inter-related causes, both social and environmental, are likely to have been involved (Seaver, 2010; Dugmore et al., 2012; Massa et al., 2012). Archaeologically- and palynologically-related radiocarbon (^{14}C) dates suggest that the Greenlandic settlement areas (Figure 1) ceased to be occupied by the end of the 15th century AD and this was certainly earlier in some areas (Arneborg et al., 1999; Edwards et al., 2011a, 2013).

Chronologies for Norse occupation sites in Greenland have been based totally on radiocarbon, biostratigraphic and artefactual dating (Gulløv et al., 2004; Edwards et al., 2011a; Schofield et al., 2013). Pollen-analytical and other palaeoenvironmental approaches have been providing unprecedentedly detailed evidence for the nature and course of Norse settlement, particularly from organic deposits lying within or in close proximity to archaeological sites (cf. Edwards et al., 2008; Buckland et al., 2009; Golding et al., 2011; Bichet et al., 2013; Ledger et al., 2013). A recurrent issue, however, has been the availability

ACCEPTED MANUSCRIPT

of suitable deposits for investigation and attendant dating problems. Mires located close to Norse ruin groups display a range of problems in that they are: (1) infrequent; (2) typically shallow with slow accumulation rates; (3) often hiatused; (4) commonly devoid of plant macro-remains other than rootlets; (5) subject to secondarily eroded inputs; and (6) rarely ombrotrophic. Lakes and ponds may provide an alternative, but allochthonous inputs and biological activity may impose dating constraints. Even the use of terrestrial macrofossils (e.g. seeds, bryophytes, charcoal) as opposed to bulk sediments has produced mixed results with frequent unconformable data, including age estimates that are clearly erroneous (Edwards et al., 2008; Edwards et al., 2011a; and see below).

For Greenland, tephras have not been sought within such anthropogenically-related deposits, unlike the situation in Iceland where visible tephras are commonplace and are an indispensable part of high precision dating control (cf. McGovern et al., 2007; Erlendsson et al., 2009; Lucas, 2009). A potential solution to the dating issues for Greenlandic investigations is to examine deposits for distal cryptotephras (far travelled volcanic ash horizons not visible to the naked eye) to provide additional chronological markers. The discovery of a number of late Holocene volcanic ash layers in Greenland ice core records (cf. Grönvold et al., 1995; Mortensen et al., 2005; Coulter et al., 2012) and the presence of cryptotephra from Alaskan and other North American eruptions located in deposits in Newfoundland (Pyne-O'Donnell et al., 2012), provide strong indications that such tephra should be evident in terrestrial deposits in Greenland. The Norse colonizers were located within three areas on the southwestern coast of Greenland (the Eastern, Middle and Western Settlements; Figure 1) and consequently they offer the opportunity to test for the presence of far-travelled ash from a number of volcanic centres. Here we present the first attempt to detect and chemically characterise distal ash associated with Norse settlement sites in Greenland and to place them in the context of radiocarbon-dated palaeoenvironmental sequences.

2. Sites and field methods

Palaeoenvironmental results are presented from three 'iconic' Norse sites in the former Eastern Settlement of Greenland (Figure 2): Herjolfsnes, Hvalsey and *Garðar* (where the modern settlement of Igaliku now stands). These were apparently amongst the locations to be settled by the first wave of colonists arriving from Iceland in AD 985 (Seaver, 2010). Further details relating to the sites, and the samples taken at each, are provided below.

2.1 Herjolfsnes

Herjolfsnes features prominently in saga literature and has attracted the widespread attention of archaeologists, largely as a consequence of Poul Nörlund's (1924) excavation of the churchyard which revealed around 200 burials, of which some were so well-preserved that items of clothing still remained intact. The ruins at Herjolfsnes comprise 10 Norse buildings, including the third largest church in Norse Greenland, a banqueting hall, a presumed byre and barn complex, and various storage buildings (Arneborg, 2006). The exposed coastal position,

ACCEPTED MANUSCRIPT

steep slopes, and an apparent lack of a good infield suggest that the site may not have been particularly well-suited for agriculture (Golding et al., 2011). It may have functioned largely as a trading post and was probably an important port of call for ships arriving in Greenland from Norway (Ingstad, 1966). In 2008, a short (~45 cm) peat monolith (Figure 2a) was collected from an eroding open section at the back of the beach ~30 m west of the churchyard wall (59°59'36.5''N, 44°43'26.3''W). The profile comprises a base of rounded (beach) cobbles overlain by a fibrous peat (45-17 cm) which becomes more humified towards the surface (17-13 cm). The peat is capped by an organic-rich sand (13-6 cm) and the modern root mat (6-0 cm). Oceanic heath dominated by *Empetrum nigrum* (crowberry) is the predominant local vegetation (plant nomenclature follows Böcher et al. (1968)).

2.2 Hvalsey

From an archaeological and historical perspective, Hvalsey is one of the most important sites in Norse Greenland. This fjord-side farmstead features the best preserved church ruins in Greenland. A marriage here in AD 1408 is the last event relating to the colony to be documented in historical records (Seaver, 2010). In addition to the church, ruins at the site include a dwelling with banqueting hall, storehouses, byre-barn complexes, and a horse paddock (Krogh, 1967; Arneborg, 2006). In 2004, a short (~30 cm) monolith was recovered from a shallow pit cut into a small (~10 m diameter) *Sphagnum*-Cyperaceae mire that is fed by a soakway ~90 m west of the banqueting hall (60°49'43.7''N, 45°47'4.7''W). The profile (Figure 2b) comprises a base of coarse sand overlain by a black, well-humified peat (26-13 cm). This grades into a poorly-humified fibrous peat (13-2 cm) which is capped by the modern root mat (2-0 cm). Vegetation around the site is predominantly heavily-grazed graminoid heath.

2.3 Igaliku

Igaliku is the location of the former cathedral and episcopal residence of the bishops of Greenland. The site was excavated by Nörlund (1929) revealing structures that include an extremely large byre with barn in which, 'there is room… [for] more than 100 cows' (ibid. p.117), together with enclosures, sheep/goat pens, warehouses and a smithy. The site is also celebrated for its system of interconnected channels and dams that formed part of a medieval irrigation network (Ingstad, 1966; Krogh, 1967; Edwards & Schofield, 2013). This appears to have been integrated with a strategy of intensive manuring of the homefield in an attempt to boost hay yields and/or buffer against periods of drought (Buckland et al., 2009). In 2005, a short (48 cm) Russian core (Jowsey 1966; 8 cm diameter) was recovered from a cirque-like basin (~72 x 48 m) on slopes above the village (60°59'25''N, 45°25'56''W); the location designated as Dam IX by Edwards & Schofield (2013). The stratigraphy (Figure 2c) comprises a solid base overlain by a pale brown sandy-clay (48-41 cm) which grades into a clay-rich gyttja (41-27 cm). This is sealed by a dark brown fibrous and well-humified peat (27-0 cm). Plant communities around the site are a mixture of grazed *Betula glandulosa-Salix glauca* (dwarf birch-willow) low scrub and managed hayfields.

ACCEPTED MANUSCRIPT

3. Laboratory methods

3.1 Palynology and dating materials

Pollen samples were prepared using standard procedures (Moore et al., 1991) including an HF stage plus the addition of an exotic marker (*Lycopodium* tablets) to enable absolute calculations. Residues were suspended in silicone oil (12,500 cSt) and each sample was counted using a Nikon E600 light microscope until a sum of 300 total land pollen (TLP) had been surpassed. Where present, microscopic charcoal particles were either measured by area (Herjolfsnes and Hvalsey) or tallied (Igaliku). Coprophilous fungal spores (van Geel et al. 2003) were also recorded.

Plant macrofossils used for radiocarbon dating were disaggregated from the peat matrix by standing overnight in a weak (<2%) NaOH solution. This was followed by gentle sieving (500 and 175 μm mesh sizes) and examination of the residues under a low power binocular microscope (8-30x magnification). Macrofossils were extracted from sieve residues using fine forceps and (prior to submission to SUERC) were stored in glass vials containing distilled water and a few drops of 10% HCl, and refrigerated. Where suitable plant macrofossils were unavailable, a small cube (~1 cm^3) of peat was submitting for dating of the humic acid fraction. These peat samples were cut directly from the cleaned surfaces of the core/monoliths.

3.2 Radiocarbon dating

Nineteen samples were submitted for AMS ^{14}C dating, consisting variously of the humic acid fraction of small (~1 cm^3) peat samples, seeds, bryophytes, bulked charcoal and wood fragments (Table 1). Pre-treatments were slight modifications of earlier methods (Stenhouse and Baxter 1983). Combustion of pre-treated samples was undertaken according to the method of Vandeputte et al. (1996). Approximately 20 mg of sample were weighed into a quartz combustion tube containing copper oxide as a source of oxygen and silver foil to mop up halides and other contaminants. The combustion tube was then evacuated, sealed and placed in a furnace at 850°C overnight. The CO_2 produced during the combustion was cryogenically purified and a 3 ml sub-sample was converted to graphite for subsequent AMS measurement using the method of Slota et al. (1987). ^{14}C measurements on graphite preparations were undertaken using a 250 kV Single Stage Accelerator Mass Spectrometer (SSAMS), manufactured by National Electrostatics Corporation. The SUERC laboratory uses SRM-4990C for all estimates of modern reference standard activity. Wheels of up to 134 samples, including standards, are measured and since measurements of such large numbers of samples can last several days, samples are measured to completion in groups of 10 in only a few hours, with Oxalic acid II primary standards spanning groups for inter-group consistency. Each group of 10 samples contains: (i) one Oxalic acid II primary standard; (ii) one humic acid secondary standard of less than one half-life in age. This sample was used in two inter-calibration exercises: C-14 Cross-check and the Fifth International Radiocarbon Intercomparison (VIRI); the consensus value from the former study is 3374 ± 9 y BP and from VIRI it is 3360 ± 3 y BP (Scott et al. 2010); (iii) either a modern secondary standard

ACCEPTED MANUSCRIPT

material [Barley mash used in the Third International Radiocarbon Intercomparison (TIRI); the consensus value from this study was 116.35 ± 0.41 pMC (Scott et al. 2003)] or a background standard (interglacial wood, infinite age bone or geological carbonate depending on the type of unknowns being measured); and (iv) seven unknowns. Each sample is automatically repeatedly measured in intra-group rotation until the sample total counting statistics and the scatter of the repeat $^{14}C/^{13}C$ measurements exceeds a quality threshold of typically 3‰.

At four levels from Herjolfsnes, paired duplicates based on different materials were also dated. Calibration of ^{14}C age estimates was performed using the IntCal13 calibration curve (Reimer et al., 2013) and Calib 7.0 (Stuiver and Reimer, 1993; Calib, 2013). Calibration of post-bomb ^{14}C samples was performed using the program CALIBomb (CALIBomb, 2013) and the Northern Hemisphere (NH) zone 1 dataset (cf. Hua and Barbetti, 2004).

3.3 Cryptotephra analyses

Samples covering the full peat profiles from the three sites were analysed for the presence of cryptotephra layers using a combination of ashing and heavy liquid centrifuge flotation with sodium polytungstate (SPT) and microscopic examination of floated and residue samples. Initial cryptotephra detection was conducted using rangefinder samples with contiguous 5 cm-long sub-samples of the highly organic peat (5 cm^3) ashed in a muffle furnace at 550 ºC for 2 hr (Pilcher and Hall, 1992). Ashed residues were also sieved between 80 μm and 15 μm to remove any coarse and fine minerogenic fractions. Sample cleaning and shard extraction used the heavy liquid centrifuge flotation method of Blockley et al. (2005) as adapted from Turney (1998). A 2.1 g/cm^3 SPT flotation density cleaned the sample of tephra-mimicking biogenic silica such as diatoms and phytoliths. This density is slightly higher than that outlined in Blockley et al. (2005) and was necessary to remove a persistent diatom presence throughout the sequences. The peat also contained an appreciable mineral component probably deriving from wind-blown material. It was therefore necessary to use SPT centrifuge flotation (2.5 g/cm^3) to float out the silicic cryptotephra glass shards from these heavier minerals. Floats were then mounted on glass slides and examined for the presence of cryptotephra shards using plane polarised light microscopy and cross-polarised light to discriminate glass from mineral grains. Rangefinders with the highest shard concentrations were then further sub-sampled at 1 cm contiguous intervals (1 cm^3 volumes) and prepared in the same manner to determine the precise stratigraphical depth of maximal shard concentrations. In order to attempt to locate basaltic shards the >2.5 g/cm^3 residues were also mounted on to slides and scanned for basaltic tephra. While painstaking this procedure has proven more successful in detecting basaltic shards in samples with very small shard concentrations than the magnetic separation technique described by Mackie et al. (2002).

Glass shards were recovered from the organic peat for WDS EPMA geochemical characterisation. Ashing cannot be used to separate shards at this stage as geochemical alteration would occur (Dugmore et al., 1995). Samples were instead subjected to a variation of the Blockley et al. (2005) method with SPT centrifuge flotation at a density of 2.1 g/cm^3.

ACCEPTED MANUSCRIPT

Although rhyolitic shards (2.4-2.5 g/cm^3; Turney, 1998) do not float at this density, the organic peat fibres will entrap shards as the rising float forms and thus prevent their separation. It was therefore necessary to retain the float in the tube and gently stir the sample between floatations in order to loosen the binding peat fibres, thus allowing shards to fall to the bottom of the tube. Care was taken to stir only the float and not the underlying column of SPT so as to avoid disturbing and re-entraining the heavier mineral component containing shards at the bottom of the tube. Up to four flotations in this manner were necessary to separate the majority of the shards from the fibrous peat matrix in the float. The float was then disposed from the tube on the final centrifuge run, followed by as many additional flotations (2.1 g/cm^3) as necessary in order to remove any remaining visible organic fraction. Rhyolitic shards were then floated from the mineral component at a density of 2.5 g/cm^3 and individual shards picked onto geochemistry stubs for sectioning and polishing. Where basaltic material had also been noted in residue scans from the rangefinder samples the > 2.5 g/cm^3 residue from the extraction for chemistry was also scanned for basaltic shards to attempt geochemical characterisation.

Where shards were successfully extracted and mounted for geochemical analyses the tephra layers were then given individual site codes based on the site abbreviation (IGA for Igaliku and HVA for Hvalsey) and their depth in the profile. Geochemical analysis by WDS EPMA was conducted at the University of Edinburgh using a CAMECA SX 100 electron microprobe. Following Hayward (2012) the accelerating voltage was 10 kev, with beam size of 5 µm and 5 nA current. Secondary standards of Lipari obsidian and BHVO-2g basalt were run alongside the unknowns to verify probe operating conditions and to check for instrument drift and these are available as supplementary online data.

4. Results

4.1 Palynology

Summary pollen diagrams for the sites are presented in Figure. 2. At Herjolfsnes (HJF) a rise in Poaceae pollen from c. 50% to in excess of 70% in HJF-2 indicates the expansion of grasslands and/or graminoid heath. This may herald the onset of *landnám*. The signature for human impact on the local environment becomes much stronger in HJF-3 (cf. Edwards et al., 2011b), where an increase in burning is indicated through an expansion in microscopic charcoal (this might be derived, at least in part, from domestic sources; cf. Edwards et al. 2008). There are also increases in *Sporormiella*-type (HdV-113) fungal spores. These are produced by a fungus that grows on animal dung (e.g. van Geel et al., 2003; Raper & Bush, 2009). Increased representation in this context seems likely to indicate the introduction of domesticated herbivores (e.g. sheep, goats, cows). The disappearance of HdV-113 spores in HJF-4, together with substantial declines in Poaceae and microscopic charcoal, suggest the cessation of farming activity with the human abandonment of the site.

At Hvalsey (HVA) the high Poaceae frequencies (c. 80%) in HVA-1, when combined with significant amounts of *Rumex acetosella* pollen (a Norse introduction; Schofield et al., 2013)

ACCEPTED MANUSCRIPT

and microscopic charcoal, indicate that the base of the profile post-dates *landnám*. A decline in Poaceae pollen and microscopic charcoal in HVA-2 and continuing through HVA-3 – a similar pattern to that observed in HJF-4 – may indicate site abandonment.

For Igaliku (IGA) the IGA-1/2 zone boundary shows a substantial decline in *Salix* pollen and the appearance and/or increase in key Norse indicators (e.g. *Rumex acetosella* and microscopic charcoal). A subsequent recovery in scrub vegetation (*Betula* and *Salix*) in IGA-3 and a decline in *R. acetosella* are suggestive of a post-Norse landscape

4.2 Radiocarbon dating

Three of the paired samples (asterisked on Figure 2; cf. Table 1) from Herjolfsnes are statistically indistinguishable with those from the same levels, while the fourth pair (38.0-37.0 cm) is virtually co-terminous (cal AD 779-1018 and 1019-1297). In addition, the similarity in ^{14}C dates throughout the Norse period (as clearly determined palynologically – see above) renders the series of little use. The 'modern' dates towards the top of the profile may reflect a possible hiatus somewhere within HJF-4.

The basal three ^{14}C dates at Hvalsey do not represent a conformable series and the upper three dates are all modern (or conceivably so for SUERC-19849). The palynology strongly suggests that Norse settlement was already extant when the basal peat began to accumulate, while a hiatus exists around the HVA-3/4 zone boundary. The radiocarbon date at the base of the sequence (SUERC-19851), if accurate, indicates that organic sediment began to accumulate during the 13th century AD

There are only two ^{14}C dates at Igaliku. As indicated palynologically (section 4.1), the age estimates are consistent with a Norse period temporal spread for zone IGA-2.

4.3 Tephrostratigraphy and tephrochronology

Figure 2 shows the results of both the 5 cm rangefinder scans and the 1 cm point sampling of all three sites. At Herjolfsnes shard concentrations were very low and thus all samples with tephra were resampled at 1cm resolution. These again yielded very low shard concentrations that were deemed too low for extraction for geochemical analyses. At two depths in the 1cm sampling single basaltic shards were identified (1 shard at 38cm and one at 40cm) and an attempt was made to isolate shards from this depth for geochemical analyses but this was unsuccessful.

The Igaliku profile suggested there was a background level of tephra deposition throughout the sequence. While this may be the result of reworking, it is more likely that this is due to the ~2000 year time period covered by the core and the number of potential eruptions that are recorded in the sequence. One sample (rangefinder 6) at a depth of 37-33 cm, yielded tephra concentrations of 55 shards in a 5 cm sample and this was re-analysed at 1cm to determine a peak. As shown in Figure 2, this peak is unimodal with maximum concentrations of 100 shards cm^{-3} at a depth of 35 cm. This sample designated IGA35 was re-extracted and prepared for chemical analyses.

ACCEPTED MANUSCRIPT

The Hvalsey profile covers a more recent timeframe and only revealed tephra in the upper rangefinder sample. This was analysed at 1cm resolution and yielded a distinct peak of 70 shards cm^{-3} at a depth of 10 cm (HVA10). The tephra designated HVA10 was re-extracted using the protocols outlined in Blockley et al. (2005) and prepared for chemical analyses.

The results of geochemical analyses of the two samples are displayed in Table 2 and summarised in Figure 3. The analyses of Igaliku tephra layer IGA35 produced major and minor chemistry for 16 vitreous tephra shards and the Hvalsey tephra HVA10 produced chemistry for 14 vitreous shards. Both tephra are sub-alkali rhyolites with SiO_2 values of 73-75 wt% and total alkali ranges of 7-7.2 wt% for HVA10 and SiO_2 values 73-79 wt% and total alkali ranges of 5.5 to 7.8 for wt% IGA35.

5. Discussion

5.1 Palynology and radiocarbon dating

At Herjolfsnes there is a clear palynological signal for Norse land use appearing in the profile, from an increase in grassland in HJF-2 through to a clear human footprint in HJF-3. Unfortunately the radiocarbon dates for Herjolfsnes do not form a consistent series. There is significant overlap in calibrated ranges across the 11th to 14th centuries AD in particular, which encompasses most of the general (conventional and accepted) timeframe for the Norse occupation of the Eastern Settlement. Thus, radiocarbon dating does not allow the precise timing of events to be determined

As was the case at Herjolfsnes, non-sequential ^{14}C dates at Hvalsey do not allow any statement about the precise timing of events. In HVA-4 and -5 there are small but distinct increases in pollen from dwarf shrubs and heaths (*Betula glandulosa* and *Salix*). The HVA-3/4 zone boundary is not particularly sharply defined, but radiocarbon dates above this returned modern (post-AD 1950) age estimates. Consequently the profile seems likely to contain a hiatus. It is tempting to equate the 'missing' part of the profile with a standstill in peat accumulation caused by the reduced temperatures of the Little Ice Age, although this assumption cannot be proven in the absence of a refined chronology for the site.

Radiocarbon dates suggest that the base of the organic part of the profile at Igaliku may extend back to ~400 cal BC. Assuming sediment accumulation was continuous thereafter, the profile should contain a Norse-age pollen record. This does appear to be the case. In this case, the timing of Norse abandonment (across IVA-2/3) based on the biostratigraphic evidence, and a radiocarbon date placed on this horizon (cal AD 1418-1618 [2σ]; SUERC-8376), appear to be in broad agreement (recalling that the conventional date for final abandonment of the Eastern Settlement falls inside the 15th century AD; cf. Berglund, 1986).

5.2 Tephrochronology

Tephra HVA10 is located above the position of a proposed hiatus at the HVA-3/4 boundary. On the basis of ^{14}C dates from this site – notably the three dates above HVA-3/4 – the tephra should be relatively modern, probably dating to as recently as the 20th century AD. Tephra IGA35 (from Igaliku) is located in the centre of LPAZ IGA-1, and thus from the

ACCEPTED MANUSCRIPT

chronological and radiocarbon discussion (above) pre-dates *landnam* (the IGA-1/2 zone boundary, on palynological grounds) possibly by several centuries. IGA35 may therefore date to a period before the first occupation of Greenland by Norse settlers and would certainly sit in the last 2400 years.

These results suggest that both sites cover the period of Norse occupation and abandonment of the region, with Igaliku potentially going further back in time. We have thus used this chronological evidence to constrain our search for possible source tephra. In order to be broad in the potential geochemical matches for these two tephra, at least to volcanic centres if not to specific eruptions, we have compared the HVA10 and IGA35 tephra to reported eruptions from potential source volcanic centres, using electron microprobe major and minor oxide data from EPMA analyses covering the last 2400 years. Details of specific publications used for comparison are given in the captions for Figures 4 to 8.

As demonstrated by Coulter et al. (2012), and based on cryptotephra studies of the Greenland ice cores, Icelandic volcanoes are likely to be a key source of tephra to Greenland in the late Holocene. This conforms to a pattern found in other studies of older time periods in the Greenland ice cores (e.g. Mortensen et al., 2005; Abbott and Davies 2012; Bourne et al., in press). Thus, we initially compared the HVA10 and IGA35 tephra chemistry to EPMA major and minor element data for Icelandic eruptions. We have used data from Tephrabase (Newton et al., 2007; http://www.tephrabase.org/) covering the last 2000 years, as well as Larsen et al., 1999, 2001, 2002; Coulter et al 2012; Gudmundsdóttir et al. 2011, 2012, and Jennings et al. 2014). The comparison with the Icelandic data is summarised in Figure 4. This suggests some similarities between HVA10 and IGA35 tephra and the reported Icelandic tephra data, but also some key differences. In Figure 4 a and b although there is some minor overlap between HVA10 and Icelandic data, FeO largely differentiates the tephra from an Icelandic source. The few points that do show some overlap are not from any particular Icelandic tephra. Tephra IGA35 is very different to the Icelandic source data, not only does it have much higher SiO_2 values but as can be seen in Figure 4 b and c it is also differentiated on Al_2O_3, and has distinctly high TiO_2 and MgO, which indicate that it has no affinity to any known Icelandic eruption. We have also compared our data to the Greenland ice core tephra for the same time period (Coulter et al., 2012). This is summarised in Figure 5 and again there is no similarity to the predominantly Icelandic tephra reported from this record. The nearest match is to the AD860 layer found in the Greenland Ice. This eruption has not been correlated to any Icelandic source, and it has been suggested that it correlates to the North American White River Ash, which has been found as a cryptotephra along the eastern seaboard of North America (Jensen et al., 2014; Pyne-O'Donnell et al., 2012).

We therefore consider that IGA35 is clearly not an Icelandic tephra, being more evolved than reported Icelandic tephra and with no clear matches on a range of paired oxide ratios. While an unknown Icelandic tephra remains a possible correlative for the HVA10 tephra, we can find no immediate obvious Icelandic candidate for this. Given the similarity (although not exact match) between HVA10 and AD860B/White River Ash, we investigated a similar source for the Greenland tephra. The HVA10 and IGA35 geochemical data were compared with a database of major and minor element chemistries of the Wrangell volcanic field

ACCEPTED MANUSCRIPT

(WVF), Aleutian Arc (AA) and Cascade and Newberry volcanoes (CA-NB) eruptions held by the University of Alberta. This is summarised in Figure 6 and the supporting information for this figure is available as supplementary information. The figure shows that IGA35, on all diagrams, has very little overlap with data from the Wrangells or Cascades, but plots within the field of the Aleutian Arc and this is investigated in more detail below. However, in consideration of the fact the Kamchatka tephra largely overlap with Aleutian tephra (c.f. van den Bogaard et al., 2014), it cannot be discounted that Kamchatka could be a source for IGA35. HVA10 overlaps with data from the Cascades in all diagrams, but also with the Wrangell field on some plots. However, when plotted with CaO, HVA10 plots more closely with the Aleutians and Cascades, with almost no overlap with the Wrangells. This suggests that the Cascades are the most likely source. This is also more likely considering the paucity of Holocene eruptions from the Wrangell volcanic field (e.g. Payne et al., 2008), but the high level of activity in the Cascades, in particular Mount St. Helens, to which HVA10 shares the most similarities.

In order to explore potential correlations in more detail we have compared IGA35 to specific Aleutian tephra in Figure 7. In this figure IGA35 is very similar to Augustine's mid-Holocene eruptions (in particular Augustine I and Augustine C). Although there is no positive correlation to any particular event for which geochemical data is available, Augustine was quite active over this period and the lack of a clear correlation could be because proximal geochemical data for these eruptions are incomplete. Nevertheless the IGA35 tephra is a much more convincing correlative of products from the Aleutians than it is from Iceland. We also explored the HVA10 tephra correlation in more detail and Figure 8 summarises the similarity of this tephra to the later Holocene eruptions of Mount St. Helens. Geochemical data included in the figure are Wn (ca. AD 1480) of “Set W”, “Layer T” (ca. 1800) of the Goat Rocks eruptive period, and the 1980 eruption (Yamaguchi, 1983). As with IGA35 there is no clear correlation to a particular eruption in the St Helens data, although there is reasonable similarity to the St Helens Wn eruption. Also included for comparison is the ‘300 cal yr BP’ event discussed by Payne et al. (2008), which has almost identical geochemistry to the White River Ash.

For both the HVA10 and IGA35 tephra, there is no clear correlation to available geochemical data, but the geochemistry of these tephra are much more similar to known eruptions from the Cascade and Aleutian Arcs than from any reported data from Iceland or the Wrangell volcanic field.

6. Conclusion

This paper reports the first examples of distal cryptotephra found in Greenlandic sedimentary contexts (i.e. deposits other than ice cores). Our data suggest that at two important Norse sites in Greenland, cryptotephra are detectable within mire sediments with shard concentrations that are practicable for geochemical analyses. The results of geochemical analyses and preliminary comparison to Icelandic and North American products indicate that the Aleutians and the Cascades are the most likely source areas for the eruptions which generated these tephra, with the Augustine and Mount St Helens volcanoes being the probable candidates.

ACCEPTED MANUSCRIPT

While this is an initial study, we view the results as important for several reasons. Firstly, the identification of two discrete tephra in sediments associated with Greenland Norse/Viking occupations sites, suggests significant potential for the future application of tephrochronology in resolving the chronological uncertainties associated with dating important archaeologically-related deposits and resolving the proposed relationship between Norse occupation of the region and late Holocene climate changes. Although we are not yet able to securely tie these tephra into dated eruptions, we are now in a position to demonstrate a proof of concept that distal cryptotephra could offer a significant advance in developing chronologies for these sites. Secondly, we have initially focused our efforts in deriving chemical analyses from the most abundant of the cryptotephra located within the Hvalsey and Igaliku sequences. There are, however, additional layers in both profiles that we will be able to investigate when new cores become available. Thirdly, and most excitingly, both of the tephra we have identified appear to correlate most closely to North American deposits and we have highlighted the two most likely source volcanoes. The Greenland ice core record suggests that there is potential for Holocene North American tephra to be deposited in Greenland (Coulter et al., 2012), with the Aniakchak tephra from Alaska reported in the mid Holocene (Hammer et al., 2003), the Mount Mazama ash recognised in the early Holocene (Zdanowicz 1999) and the White River Ash in the Late Holocene (Jensen et al., 2014). Nevertheless, the predominant source for Greenland ice core tephra is the Icelandic volcanic province (Abbott and Davies 2012; Davies et al., 2014). Our data suggest that in the southwest of Greenland it may be more common for tephra to be sourced from North American volcanoes, which also opens up the possibility of more North American tephra becoming a source for correlating between North America and the North Atlantic region.

Finally, the application of cryptotephra studies to palaeoenvironmental sequences means that there is significant potential to include additional direct chronological information into palaeoenvironmental records that also contain proxies both for a human presence and an environmental response (to e.g. climate forcing). This may allow us to refine the chronologies associated with Norse activities in Greenland (e.g. abandonment) as recorded in palaeoenvironmental archives. We also note that cryptotephra investigations within Holocene deposits both in Greenland, the North Atlantic and eastern North America are at a relatively early stage. Full analyses of cryptotephra from the Greenland ice cores is not yet complete, and there is very limited research from the western North Atlantic or the North American mainland away from regional volcanic centres. It seems likely that the potential demonstrated here will lead to the incorporation of Norse palaeoenvironmental sequences into a regional tephrostratigrapic framework for correlating palaeoenvironmental transitions, as with the much more developed records from the eastern North Atlantic region.

Acknowledgements

ACCEPTED MANUSCRIPT

The Leverhulme Trust are thanked for the funding of fieldwork. Paul Buckland, Eva Panagiotakopulu and Andy McMullen assisted with the collection of samples, Fiona Thompson with palynology at Igaliku, and Alison Sandison with artwork. Support to DF and BJ is provided by grants from the Natural Science and Engineering Research Council of Canada. We are also very grateful for the useful comments and advice of an anonymous referee.

ACCEPTED MANUSCRIPT

ACCEPTED MANUSCRIPT

References

Abbott, P.M., Davies, S.M., 2012. Volcanism and the Greenland ice-cores: the tephra record. Earth-Sci Rev 115, 173-191.

Arneborg, J., Heinemeier, J., Lynnerup, N., Nielsen, H.L., Rud, N., Sveinbjörnsdóttir ÁE. 1999. Change of diet of the Greenland Vikings determined from stable carbon isotope analysis and 14C dating of their bones. Radiocarbon 41, 157–68.

Arneborg, J. 2006. Saga trails – Brattahlið, Garðar, Hvalsey Fjord's Church and Herjolfsnes: four chieftain's farmsteads in the Norse settlement of Greenland. A visitor's guidebook. National Museum of Denmark, Nanortalik Museum, Narsaq Museum and Qaqortoq Museum.

Berglund, J. 1986. The decline of the Norse Settlements in Greenland. Arctic Anthropology 23, 109–135.

Bichet, V., Gauthier, E., Massa, C., Perren, B., Richard, H., Petit, C., Mathieu, O. 2013. The history and impacts of farming activities in south Greenland: an insight from lake deposits Polar Record 49, 210–220.

Blockley, S.P.E., Pyne-O'Donnell, S.D.F., Lowe, J.J., Matthews, I.P., Stone, A., Pollard, A.M., Turney, C.S.M., Molyneux, E.G. 2005. A new and less destructive laboratory procedure for the physical separation of distal glass tephra shards from sediments. Quaternary Science Reviews 24, 1952-1960.

Böcher T.W., Holmen K., Jakobsen K. 1968. The flora of Greenland. P. Haase & Son, Copenhagen.

Bourne, A.J., Cook, E., Abbott, P.M., Seierstad, I.K., Steffensen, J.P., Svensson, A., Fischer, H., Scupbach, S., Davies, S.M. in press. A tephra lattice for Greenland and a reconstruction of volcanic events spanning 25-45 ka b2k. Quaternary Science Reviews doi:10.1016/j.quascirev.2014.07.017

Boygle, J.E. 1994. Tephra in lake sediments: an unambiguous geochronological marker? PhD Thesis, University of Edinburgh.

Buckland, P.C., Edwards, K.J., Panagiotakopulu, E., Schofield, J.E. 2009. Palaeoecological evidence for manuring and irrigation at *Garðar* (Igaliku), Norse Eastern Settlement, Greenland. The Holocene 19, 105–116.

CALIB. 2013. http://calib.qub.ac.uk/calib. Accessed: November 2013.

CALIBomb. 2013. http://intcal.qub.ac.uk/CALIBomb/tinycalib.html. Accessed: November 2013.

Coulter, S.E., Pilcher, J.R., Plunkett, G., Baillie, M., Hall, V.A., Steffensen, J.P., Vinther, B.M., Clausen, H.B., Johnsen, S.J. 2012. Holocene tephras highlight complexity of volcanic

ACCEPTED MANUSCRIPT

signals in Greenland ice cores. Journal of Geophysical Research 117, D21303, doi:10.1029/2012JD017698.

Dugmore, A.J., McGovern, T.H., Vésteinsson, O., Arneborg, J., Streeter, R., Keller, C. 2012. Cultural adaptation, compounding vulnerabilities and conjunctures in Norse Greenland. Proceedings of the National Academy of Sciences 109, 3658-3663.

Dugmore, A.J., Church, M.J., Buckland, P.C., Edwards, K.J., Lawson, I., McGovern, T.H., Panagiotakopulu, E., Simpson, I.A., Skidmore, P., Sveinbjarnardóttir, G. 2005. The Norse *landnám* on the North Atlantic islands: an environmental impact assessment. Polar Record 41, 21–37.

Dugmore, A.J., Larsen, G., Newton, A.J. 1995. Seven tephra isochrones in Scotland. The Holocene 5, 257-266.

Edwards, K.J., Schofield, J.E., Mauquoy, D. 2008. High resolution paleoenvironmental and chronological investigations of Norse *landnám* at Tasiusaq, Eastern Settlement, Greenland. Quaternary Research 69, 1-15.

Edwards, K.J., Schofield, J.E., Kirby, J.R., Cook, G.T. 2011a. Problematic but promising ponds? Palaeoenvironmental evidence from the Norse Eastern Settlement of Greenland. Journal of Quaternary Science 26, 854–865.

Edwards, K.J., Erlendsson, E., Schofield, J.E. 2011b. Is there a Norse 'footprint' in North Atlantic pollen records? In: Sigmundsson, S., Holt, A., Sigurðsson, G., Ólafsson, G., Vésteinsson, O. (eds) Viking settlements and society: papers from the Sixteenth Viking Congress, Reykjavík and Reykholt, 16-23 August 2009. Hið íslenska fornleifafélag and University of Iceland Press, Reykjavík, 65–82.

Edwards, K.J., Schofield, J.E., Cook, G.T., Nyegaard, G. 2013. Towards a first chronology for the Middle Settlement of Norse Greenland: ^{14}C and related studies of animal bone and environmental material. Radiocarbon 55, 13-29

Edwards, K.J., Schofield, J.E. 2013. Investigation of proposed Norse irrigation channels and dams at *Garðar*/Igaliku, Greenland. Water History 5, 71-92.

Erlendsson, E., Edwards, K.J., Buckland, P.C. 2009. Vegetational response to human colonisation of the coastal and volcanic environments of Ketilsstaðir, southern Iceland. Quaternary Research 72, 174-187.

Fitzhugh, W.W, Ward E.I. (eds). 2000. Vikings: the North Atlantic Saga. Smithsonian Books, Washington.

Golding, K.A., Simpson, I.A., Schofield, J.E., Edwards, K.J. 2011. Norse-Inuit interaction and landscape change in southern Greenland? A geochronological, pedological and palynological investigation. Geoarchaeology 26, 315–45.

ACCEPTED MANUSCRIPT

Grönvold, K., Oskarsson, N., Johnsen, S.J., Clausen, H.B., Hammer, C.U., Bond, G., Bard, E. 1995. Ash layers from Iceland in the Greenland GRIP ice core correlated with oceanic and land sediments. Earth and Planetary Science Letters 135 149–155.

Grove, J.M. 1988. The Little Ice Age. Routledge, London.

Gudmundsdóttir, E.R., Larsen, G and Eiriksson, J. 2011. Two new Icelandic tephra markers: The Hekla O tephra layer, 6060 cal. yr BP, and Hekla DH tephra layer, similar to 6650 cal. yr BP. Land-sea correlation of mid-Holocene tephra markers. Holocene 21, 629-639.

Gudmundsdóttir, E.R., Larsen, G and Eiriksson, J. 2012. Tephra stratigraphy on the North Icelandic shelf: extending tephrochronology into marine sediments off North Iceland. Boreas 41, 718-734.

Gulløv, H.C., Andreason, C., Grønnow, B., Jensen, J.F., Appelt, M., Arneborg, J., Berglund, J. 2004. Grønlands Forhistorie. Gyldendal, Copenhagen.

Hall, V.A., Pilcher, J.R. 2002. Late-Quaternary Icelandic tephras in Ireland and Great Britain: detection, characterization and usefulness. The Holocene 12, 223-230.

Hammer, C.U., Kurat, G., Hoppe, P., Grum, W., Clausen, H.B., 2003. Thera eruption date 1645 BC confirmed by new ice core data? In: Bietak, M. (Ed.), The Synchronisation of Civilisations in the Eastern Mediterranean. Austrian Academy of Science, Vienna, pp. 87–94.

Hannon, G.E., Hermanns-Audardottir, M., Wastegard, S. 1998. Human impact at Tjornuvik in the Faroe Islands. Frodskaparrit 46, 215-228.

Hayward, C. 2012. High spatial resolution electron probe microanalysis of tephras and melt inclusions without beam-induced chemical modification. Holocene 22, 119-125.

Hua, Q., Barbetti, M. 2004. Review of tropospheric bomb ^{14}C data for carbon cycle modeling and age calibration purposes. Radiocarbon 46, 1273-1298.

Ingstad, H. 1966. Land under the Pole Star. Jonathan Cape, London.

Irvine, T.N., Barager, W.R.A., 1971, A Guide to the Chemical Classification of the Common Volcanic Rocks. Canadian Journal of Earth Sciences, 8: 523-548, 10.1139/e71-055

Jennings, A., Thordarson, T., Zalzal, K., Stoner, J., Hayward, C., Geirsdóttir, A., Miller, G. 2014Holocene tephra from Iceland and Alaska in SE Greenland Shelf Sediments. Geological Society, London, Special Publications, 398 doi:10.1144/SP398.6.

Jensen, B.J.L., Pyne-O'Donnell, S., Plunkett, G., Froese, D.G., Hughes, P.D.M, Sigl, M., McConnell, J.R., Amesbury, M., Blackwell, P.G., van den Bogaard, C., Buck, C., Charman, D.J., Clague, J.J., Hall, V.A., Koch, J., Mackay, H., Mallon, G., McColl, L., Pilcher, J.R., 2014. Transatlantic correlation of the Alaskan White River Ash. Geology, 42, 875-878.

ACCEPTED MANUSCRIPT

Jowsey, P.C. 1966. An improved peat sampler. New Phytologist 65, 245–248.

Krogh, K.J. 1967. Viking Greenland. The National Museum, Copenhagen.

Larsen, G. 2000. Holocene eruptions within the Katla volcanic system, south Iceland: Characteristics and environmental impact. Jokull 49, 1-28.

Larsen, G., Dugmore, A.J., Newton, A.J. 1999. Geochemistry of historic silicic tephras in Iceland. The Holocene 9, 463-471.

Larsen, G., Eiriksson, J., Knudsen, K.L. and Heinemeier, J. 2002. Correlation of late Holocene terrestrial and marine tephra markers, north Iceland: implications for reservoir age changes. Polar Research 21, 283-290.

Larsen, G., Newton, A.J., Dugmore, A.J. and Vilmundardottir, E. 2001. Geochemistry, dispersal, volumes and chronology of Holocene silicic tephra layers from the Katla volcanic system, Iceland. Journal of Quaternary Science 16, 119-132.

Le Bas, M.J., Le Maitre, R.W., Streckeisen, A., Zanettin, B. 1986. A chemical classification of volcanic rocks based on the total alkali–silica diagram. Journal of Petrology 27, 745–750.

Ledger, P.M., Edwards, K.J., Schofield, J.E. 2013. Shieling activity in the Norse Eastern Settlement: palaeoenvironmental evidence from the 'Mountain Farm', Vatnahverfi, Greenland. The Holocene 23, 810-822.

Lucas, G. 2009. Hofstaðir: excavations of a Viking Age feasting hall in North-Eastern Iceland. Reykjavik: Institute of Archaeology Monograph Series 1.

MacDonald, G.A., Katsura, T., 1964. Chemical composition of Hawaiian lavas. Journal of Petrology 5, 83e133.

Mackie, E., Turney, C., Dobbyn, K., Lowe, J., Hill, P., Davies, S. 2002. The use of magnetic separation techniques to detect basaltic microtephra in last glacial-interglacial transition (LGIT; 15-10 ka cal. BP) sediment sequences in Scotland. SCOTTISH JOURNAL OF GEOLOGY 38, 21-30.

Massa, C., Bichet, V., Gauthier, E., Perren, B.B., Mathieu, O., Petit, C., Monna, F., Giraudeau, J., Losno, R., Richard, H. 2012. A 2500 year record of natural and anthropogenic soil erosion in south Greenland. Quaternary Science Reviews 32, 119–130.

McGovern, T.H., Vésteinsson, O., Friðriksson, A., Church, M., Lawson, I., Simpson, I.A., Einarsson, A., Dugmore, A., Cook, G., Perdikaris, S., Edwards, K.J., Thomson, A., Adderley, W.P., Newton, A., Lucas, G., Edvardsson, R., Aldred, O., Dunbar, E. 2007. Landscapes of settlement in Northern Iceland: historical ecology of human impact and climate fluctuation on the millennial scale. American Anthropologist 109, 27-51.

Moore, P.D., Webb, J.A., Collinson, M.E. 1991. Pollen analysis, 2nd edition. Blackwell, Oxford.

ACCEPTED MANUSCRIPT

Mortensen, A.K., Bigler, M., Grönvold, K., Steffensen, J.P., Johnsen, S.J. 2005. Volcanic ash layers from the Last Glacial Termination in the NGRIP ice core. Journal of Quaternary Science 20, 209-219.

Newton, A.J., Dugmore, A.J. and Gittings, B.M. (2007) Tephrabase: tephrochronology and the development of a centralised European database. Journal of Quaternary Science 22, 737-743.

Nörlund, P. 1924. Buried Norsemen at Herjolfsnes. Meddelelser om Grønland 67, 1-270.

Nörlund. P. 1929. Norse ruins at Gardar: the episcopal seat of mediaeval Greenland. Meddelelser om Grønland 76, 1-171.

Oldfield, F., Thompson, R., Crooks, P.R.J., Gedye, S.J., Hall, V.A., Harkness, D.D., Housley, R.A., McCormac, F.G., Newton, A.J., Pilcher, J.R., Renberg, I., Richardson, N. 1997. Radiocarbon dating of a recent high-latitute peat profile: Stor Amyran, northern Sweden. The Holocene 7, 283-290.

Payne, R., Blackford, J., van der Plicht, J. 2008. Using cryptotephras to extend regional tephrochronologies: an example from southeast Alaska and implications for hazard assessment. Quaternary Research 69, 42–55.

Pilcher, J.R., Hall V.A. 1992. Towards a tephrochronology for the Holocene for the north of Ireland. The Holocene 2, 255-260.

Pilcher, J.R., Hall, V.A., McCormac, F.G. 1995. Dates of Holocene Icelandic volcanic eruptions from tephra layers in Irish peats. The Holocene 5, 103-110.

Pilcher, J.R., Hall, V.A., McCormac, F.G. 1996. An outline tephrochronology for the Holocene of the north of Ireland. Journal of Quaternary Science 11, 485-494.

Pyne-O'Donnell, S.D.F, Hughes P.D.M., Froese, D.G., Jensen, B.J.L., Mallon, G., Amesbury, M.J., Daley, T.J., Charman, D.J., Street-Perrott, F.A., Loader, N.J., Woodman-Ralph, J., Mauquoy, D. 2012. High-precision ultra-distal Holocene tephrochronology in North America. Quaternary Science Reviews 52, 6-11.

Raper, D., Bush, M. 2009. A test of *Sporormiella* representation as a predictor of megaherbivore presence and abundance. Quaternary Research 71, 490-496.

Reimer, P.J., Bard, E., Bayliss, A., Beck, J.W., Blackwell, P.G., Bronk Ramsey, C., Buck, C.E., Cheng, H., Edwards, R.L., Friedrich, M., Grootes, P.M., Guilderson, T.P., Haflidason, H., Hajdas, I., Hatté, C., Heaton, T.J., Hogg, A.G., Hughen, K.A., Kaiser, K.F., Kromer, B., Manning, S.W., Niu, M., Reimer, R.W., Richards, D.A., Scott, E.M., Southon, J.R., Turney, C.S.M., van der Plicht, J. 2013. IntCal13 and Marine13 radiocarbon age calibration curves 0-50,000 years cal BP. Radiocarbon 55, 1869-1887.

Schofield, J.E., Edwards, K.J., Erlendsson, E., Ledger, P.M. 2013. Palynology supports 'Old Norse' introductions to the flora of Greenland. Journal of Biogeography 40, 1119-1130.

ACCEPTED MANUSCRIPT

Scott, E.M. 2003. The third international radiocarbon intercomparison (TIRI). Radiocarbon 45, 293-328.

Scott, E.M., Naysmith, P. and Cook, G.T. 2010. VIRI – summary results and overall assessment. Radiocarbon 52, 859-865.

Seaver, K.A. 2010. The last Vikings: the epic story of the great Norse voyagers. I.B. Tauris, London.

Slota, P.J., Jull, A.J.T., Linick, T.W., Toolin, L.J. 1987. Preparation of small samples for ^{14}C accelerator targets by catalytic reduction of CO. Radiocarbon 29, 303–306.

Stenhouse, M J., Baxter, M.S. 1983. ^{14}C dating reproducibility: evidence from routine dating of archaeological samples. PACT 8, 147–61.

Stuiver, M., Reimer, P. J. 1993. Extended ^{14}C database and revised CALIB radiocarbon calibration program. Radiocarbon 35, 215-230.

Turney, C.S.M. 1998. Extraction of rhyolitic component of Vedde microtephra from minerogenic lake sediments. Journal of Paleolimnology 19, 199-206.

van den Bogaard, C., Jensen, B. J. L., Pearce, N. J. G., Froese, D. G., Portnyagin, M. V., Ponomareva, V. V., Wennrich, V., 2014. Volcanic ash layers in Lake El'gygytgyn: eight new regionally significant chronostratigraphic markers for western Beringia. Climate of the Past, 10, 1041–1062. doi:10.5194/cp-10-1041-2014-supplement

van Geel, B., Buurman, J. Brinkkemper, O., Schelvis, J., Aptroot, A., van Reenen, G., Hakbijl, T. 2003. Environmental reconstruction of a Roman Period settlement site in Uitgeest (The Netherlands), with special reference to coprophilous fungi. Journal of Archaeological Science 30, 873-883.

Vandeputte, K., Moens, L., Dams, R. 1996. Improved sealed-tube combustion of organic samples to CO_2 for stable isotope analysis, radiocarbon dating and percent carbon determinations. Analytical Letters 29, 2761–2773.

Wastegard, S. 2002. Early to middle Holocene silicic tephra horizons from the Katla volcanic system, Iceland: new results from the Faroe Islands. Journal of Quaternary Science 17, 723-730.

Wastegard, S., Bjorck, S., Grauert, M., Hannon, G.E. 2001. The Mjauvotn tephra and other Holocene tephra horizons from the Faroe Islands: a link between the Icelandic source region, the Nordic Seas, and the European continent. The Holocene 11, 101-109.

Yamaguchi, D.K., 1983. New tree-ring dates for recent eruptions of Mount St. Helens. Quaternary Research 20, 246–250.

Zdanowicz, C.M., Zielinski, G.A., Germani, M.S., 1999. Mount Mazama eruption: calendrical age verified and atmospheric impact assessed. Geology 27, 621-624.

ACCEPTED MANUSCRIPT

Figure captions

Figure 1: Locations of the three field sites within the Norse Eastern Settlement of southern Greenland featured in this study. Inset (top right): the Eastern (E), Middle (M) and Western (W) Settlements (boxed). Inset (bottom left): locations of major volcanic centres mentioned in the text, depicted relative to Greenland.

Figure 2: Percentage pollen diagrams for the three field sites (A, Herjolfsnes; B, Hvalsey; C, Igaliku) displaying key selected taxa and associated proxies plotted against peaks in cryptotephra. Local pollen assemblage zones (prefixed HJF, HVA and IGA) are discussed in the text. For Herjolfsnes and Hvalsey, charcoal is presented as the ratio of charcoal to pollen concentration (C:P). For Igaliku, charcoal data are presented as percentages of particulates (calculated against the TLP sum). Radiocarbon dates are displayed using their 2σ (cal BC/AD) calibrated ranges. The vertical resolution (thickness) of each ^{14}C sample is 1 cm. The asterisks at Herjolfsnes denote paired ^{14}C samples (cf. Table 1). The shaded areas within local pollen assemblage zones HJF-4 at Herjolfsnes and HVA-3 at Hvalsey are possible hiatus levels. Tephra shard counts (shards cm^{-3}) for the 5 cm rangefinder samples and 1 cm point samples are also shown.

Figure 3: (a) Summary TAS (Le Bas et al., 1986) diagram for the IGA35 and HVA10 tephra samples indicating that both are highly silicic subalkaline rhyolites; (b) an AFM (Alkali, FeO* = total Fe as FeO, MgO) after Irvine and Baragar (1971) and (c) a biplot based on the alkaline/subalkanie division of MacDonald and Katsura (1964).

Figure 4: Harker variation diagram of SiO_2 against Al_2O_3, TiO_2, FeOt and MgO wt% for IGA35 and HVA10 tephra against reported Late Holocene tephra from Iceland (data from Tephrabase and additional sources, Boygle 1994; Coulter et al., 2012; Dugmore et al., 1995; Pilcher et al., 1995, 1996; Oldfield et al., 1997; Hannon et al., 1998; Larsen et al., 1999, 2001; 2002; Larsen 2000; Wastegard et al., 2001; Hall and Pilcher 2002; Wastegard, 2002; Gudmundsdottir et al., 2011, 2012; Jennings et al., 2014). Only data from Iceland with SiO_2 values greater than 70 wt% are shown as this is below the minimum SiO_2 concentrations in either IGA35 and HVA10.

Figure 5: IGA35 and HV10 compared to tephra geochemical data from the Greenland ice cores (Coulter et al 2012) for the last two millennia. Squares = QUB-1528 (AD860B/White River Ash, eastern lobe); triangle = QUB-1052 (Öraefajökull, AD 1362/63); upside-down triangle = QUB-1004 (Katmai, AD 1912/13); grey cross = QUB-1303/04 (unknown, AD 1364); blue cross (X) = QUB 1212/13 (unknown, AD 931): yellow cross = QUB-1539 (unknown, 2300-2298 BC); star = QUB-1437 (unknown, AD 941/42); diamond = QUB-1425 (unknown, AD 953/54)

Figure 6: Harker diagrams of compiled data from the Wrangell volcanic field (WVF), Aleutian Arc (AA) and Cascade and Newberry volcanoes (CA-NB) in comparison to unknowns. Details on the sources for the data compilation are included in supplementary materials. Only data with SiO_2 values greater than 70 wt% are shown as this is below the minimum SiO_2 concentrations in either IGA35 and HVA10.

ACCEPTED MANUSCRIPT

Figure 7: IGA35 compared with glass geochemical data from mid-Holocene eruptions from Augustine volcano. The data is limited to material over 74 wt%. Also included for comparison is NDN 260 (Pyne-O'Donnell et al., 2012), which was originally tentatively correlated to Augustine G, although new data suggests this is not the case.

Figure 8: HV10 compared to the later Holocene Mount St. Helen's data. Geochemical data included in the figure are Wn (ca. AD 1480) of "Set W", "Layer T" (ca. 1800) of the Goat Rocks eruptive period, and the 1980 eruption (Yamaguchi, 1983). Also included for comparison is the "300 cal yr BP" event discussed by Payne et al. (2008), which has almost identical geochemistry to the White River Ash.

Table 1: Radiocarbon dates from Herjolfsnes, Hvalsey, and Igaliku.

Table 2: Results of WDS-EPMA analyses of single shards from the IGA35 and HVA10 tephra. See text for details of the EPMA operating conditions.

ACCEPTED MANUSCRIPT

Figure 1

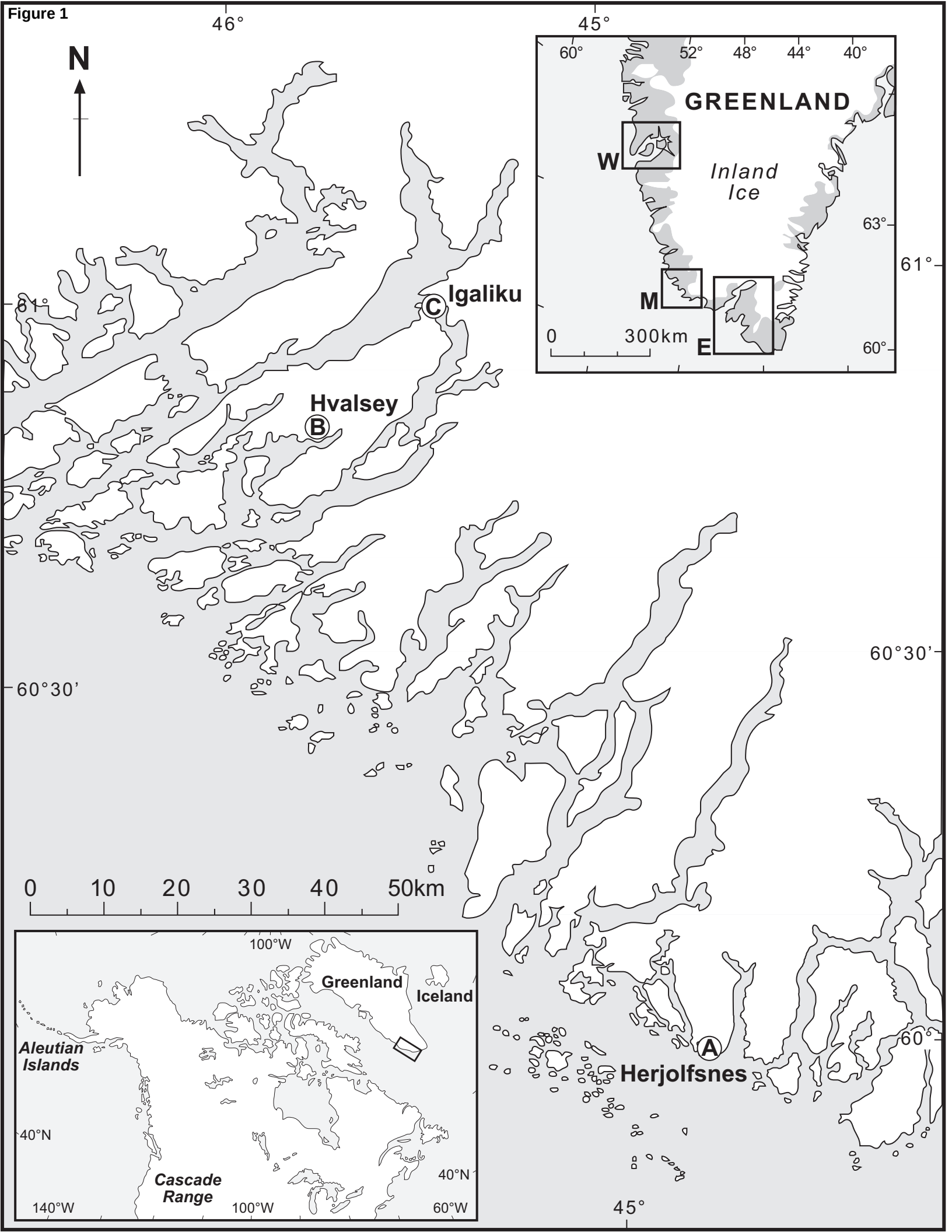
46°
45°
N
60°
52°
48°
44°
40°
GREENLAND
W
Inland
Ice
63°
61°
M
E
0
300km
60°
61°
Igaliku
C
Hvalsey
B
60°30'
60°30'
0
10
20
30
40
50km
100°W
Greenland
Iceland
Aleutian
Islands
40°N
Cascade
Range
40°N
140°W
100°W
60°W
A
Herjolfsnes
60°
45°

ACCEPTED MANUSCRIPT

Figure 2

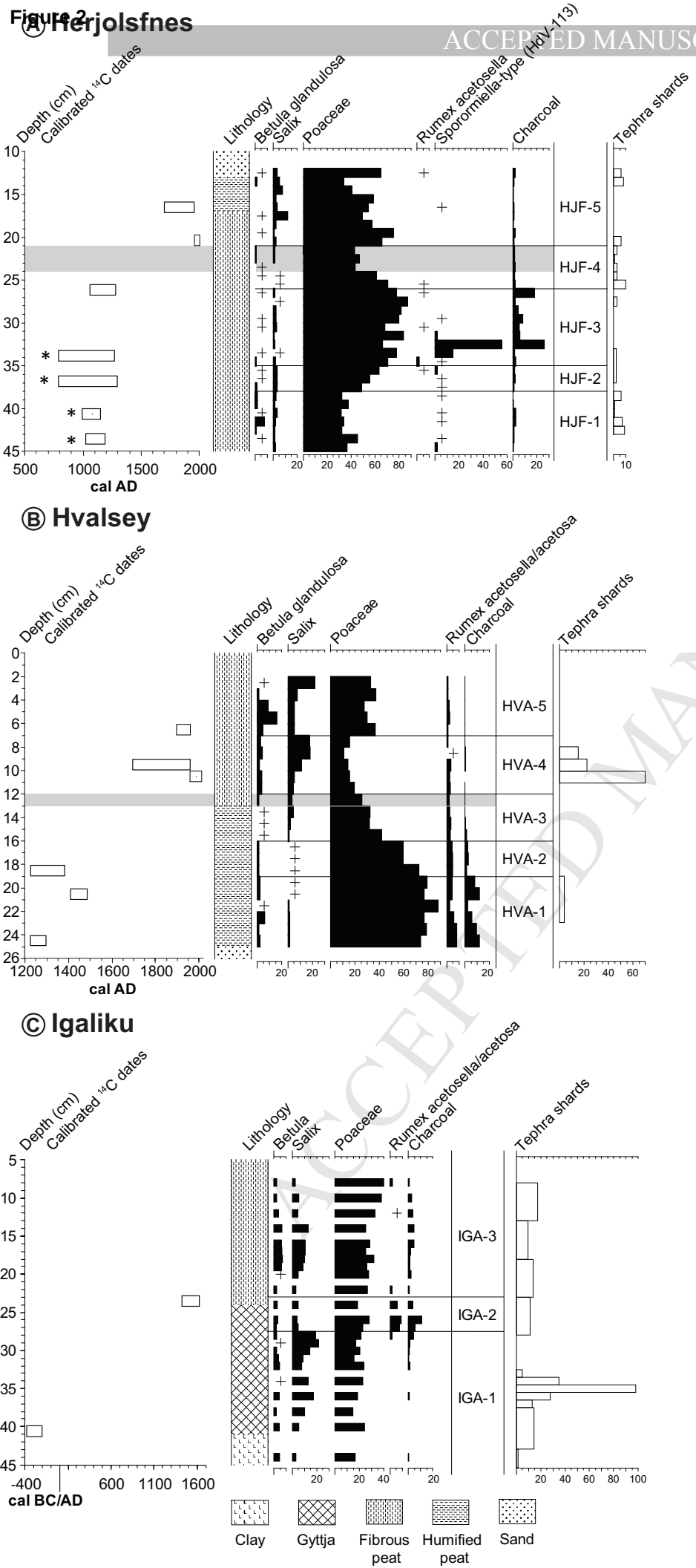

Figure 3a

ACCEPTED MANUSCRIPT

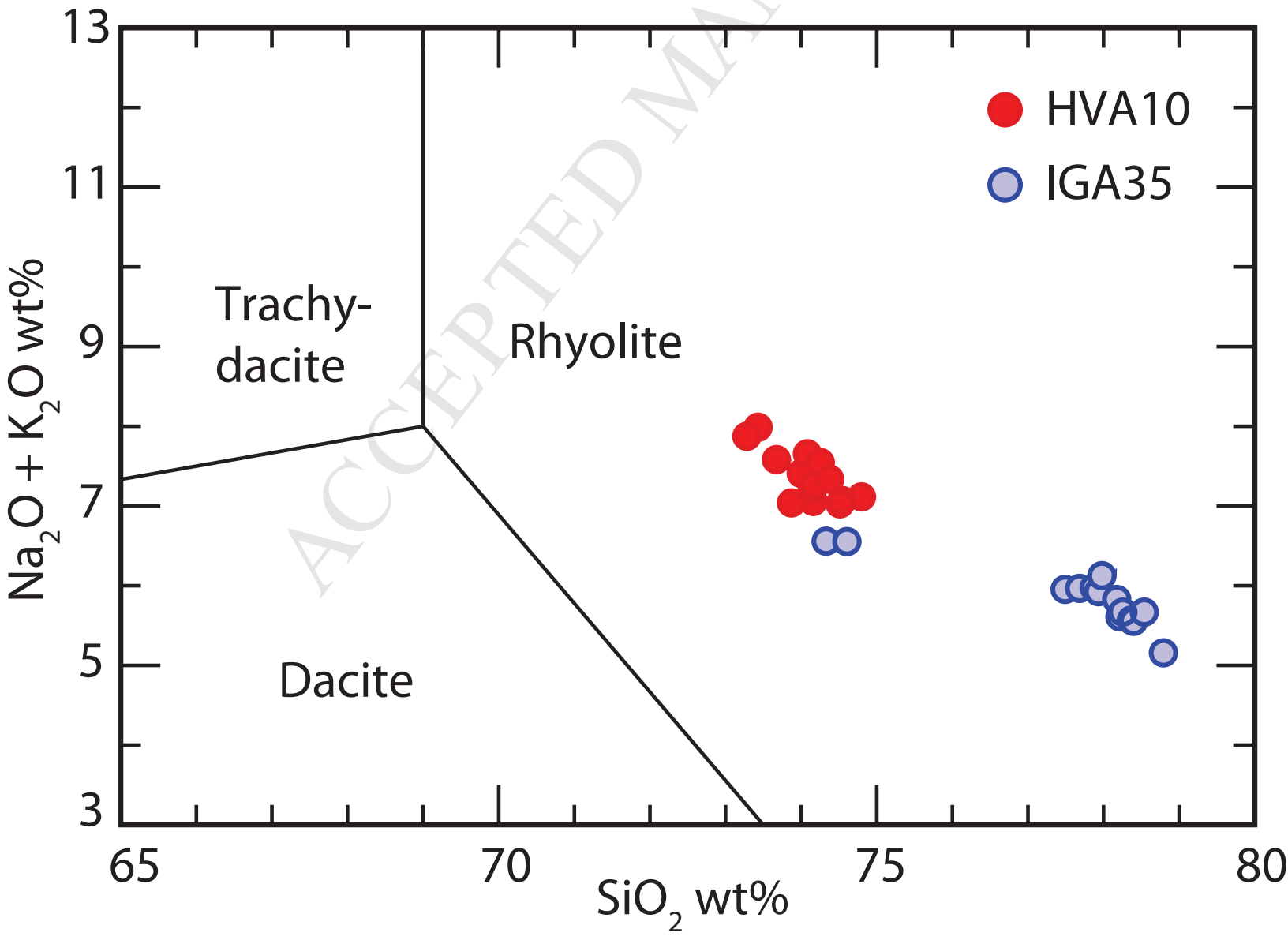

ACCEPTED MANUSCRIPT

Figure 3b

ACCEPTED MANUSCRIPT

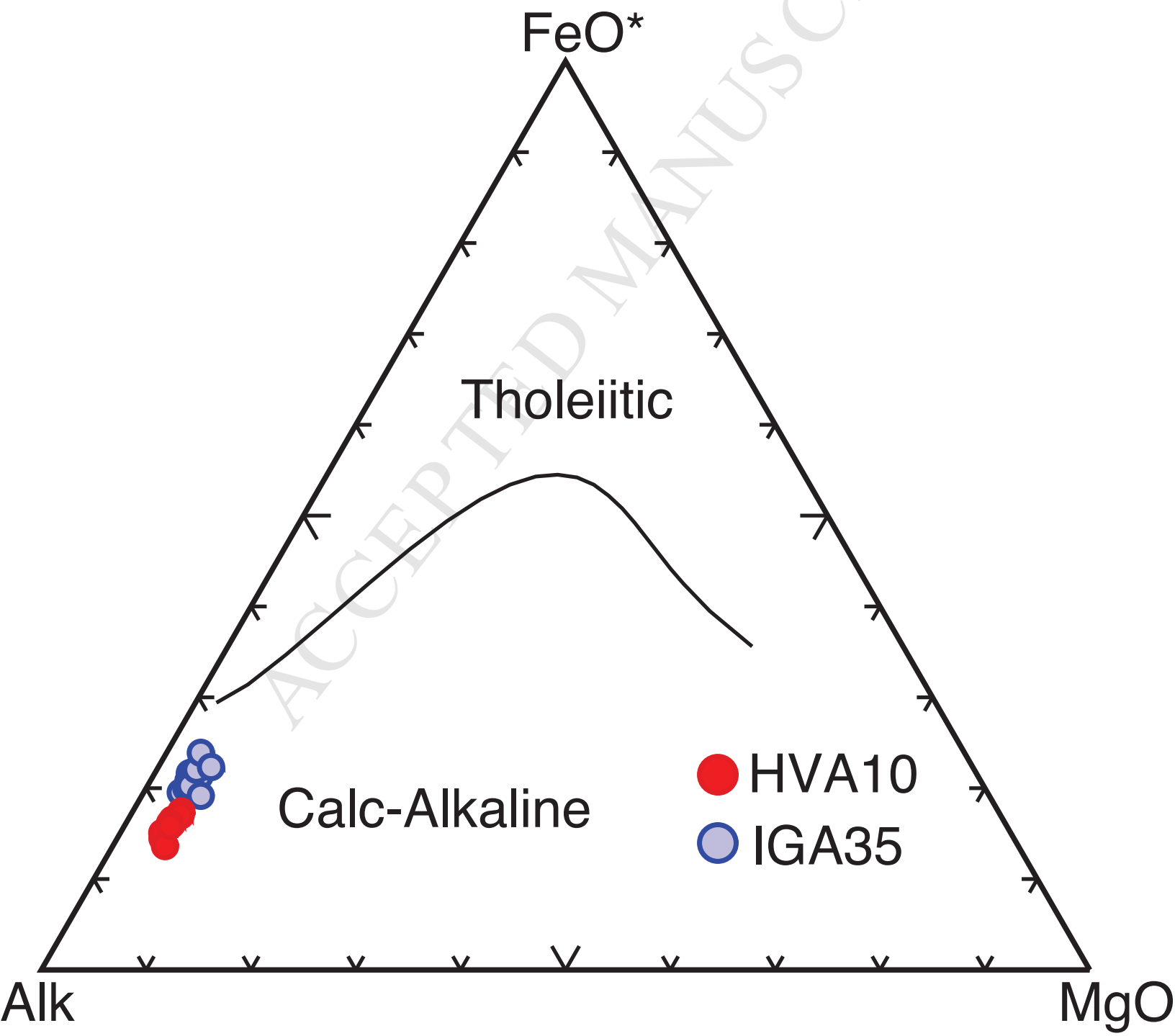

ACCEPTED MANUSCRIPT

Figure 3c

ACCEPTED MANUSCRIPT

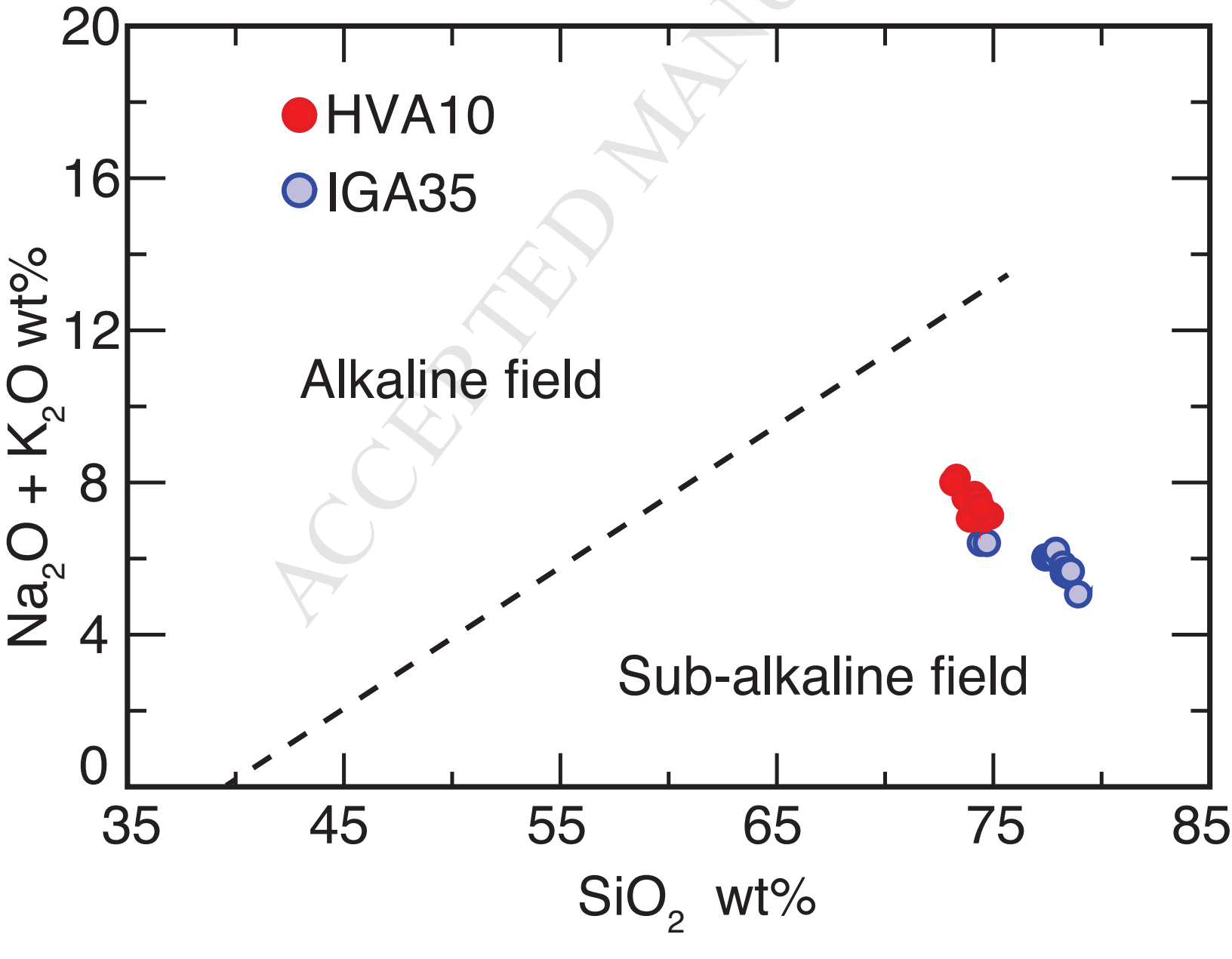

ACCEPTED MANUSCRIPT

Figure 4

ACCEPTED MANUSCRIPT

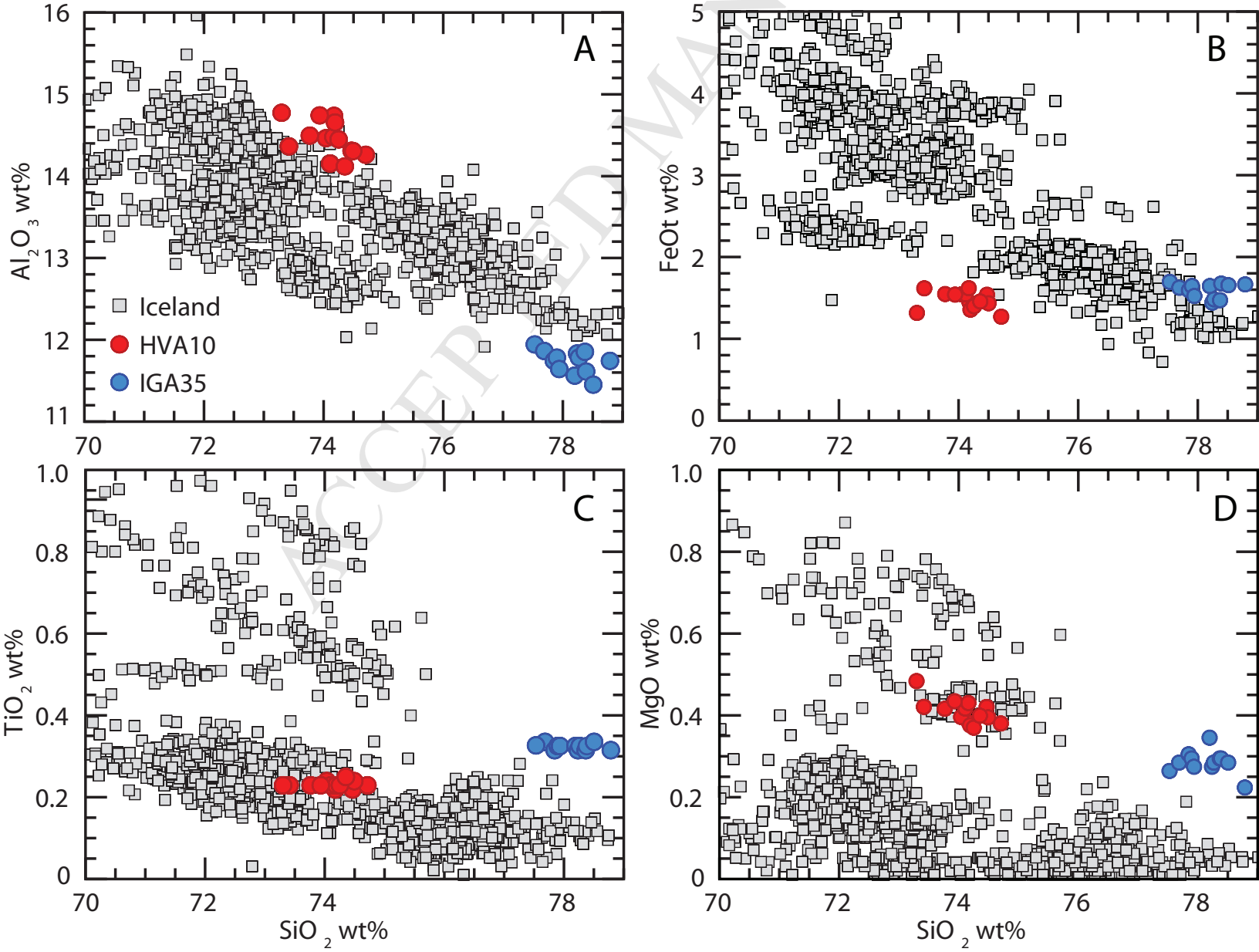

ACCEPTED MANUSCRIPT

Figure 5

ACCEPTED MANUSCRIPT

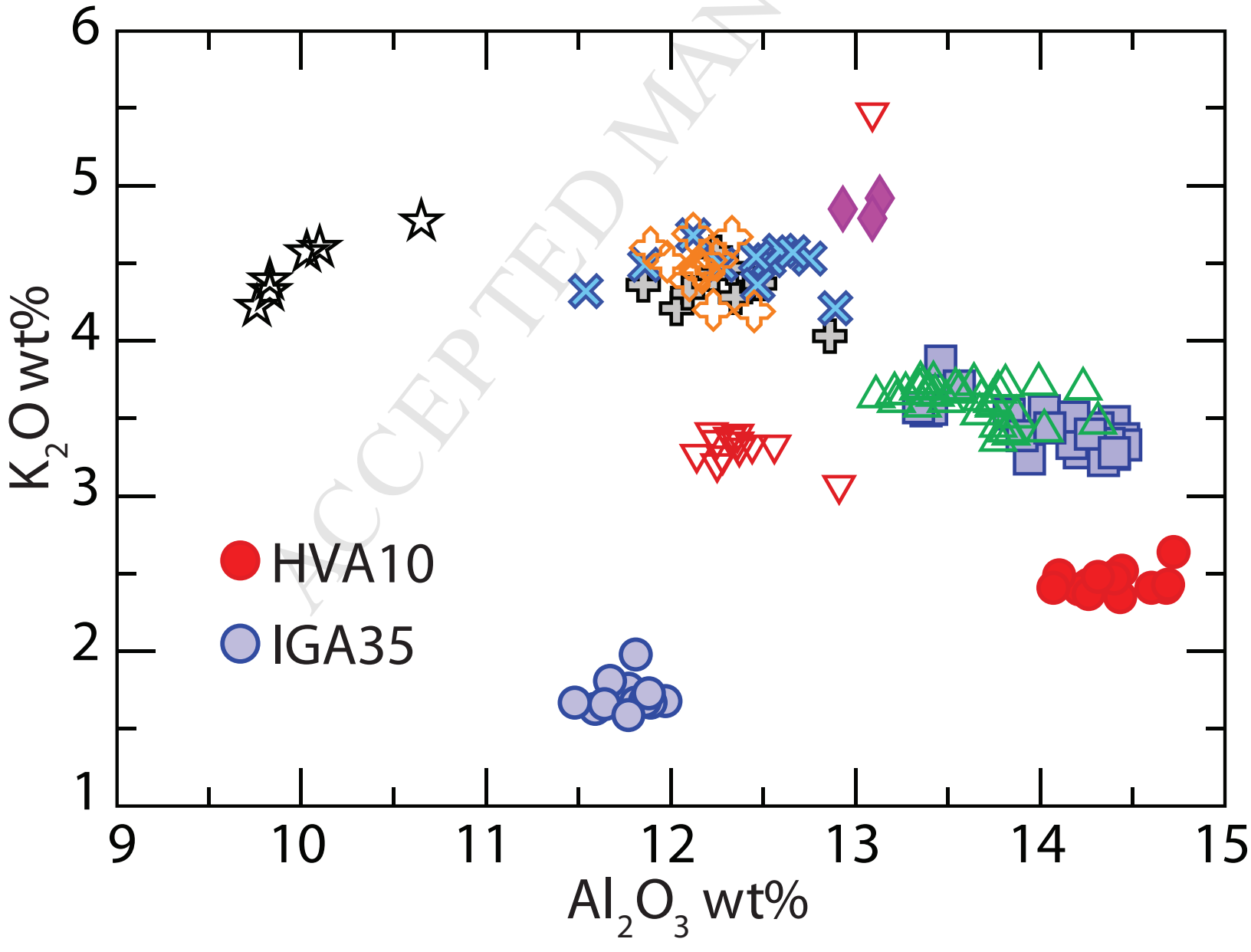

ACCEPTED MANUSCRIPT

Figure 6

ACCEPTED MANUSCRIPT

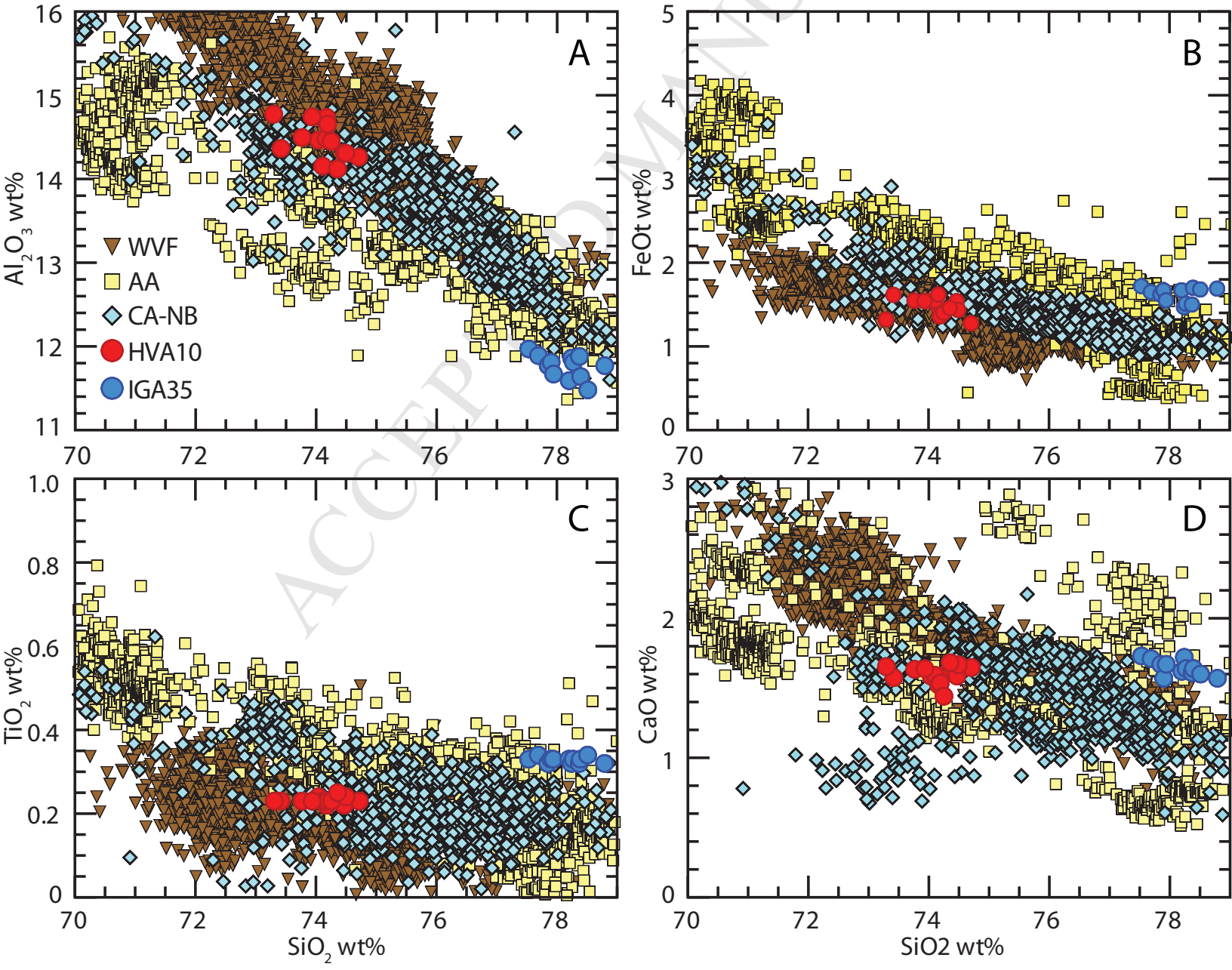

Figure 7

ACCEPTED MANUSCRIPT

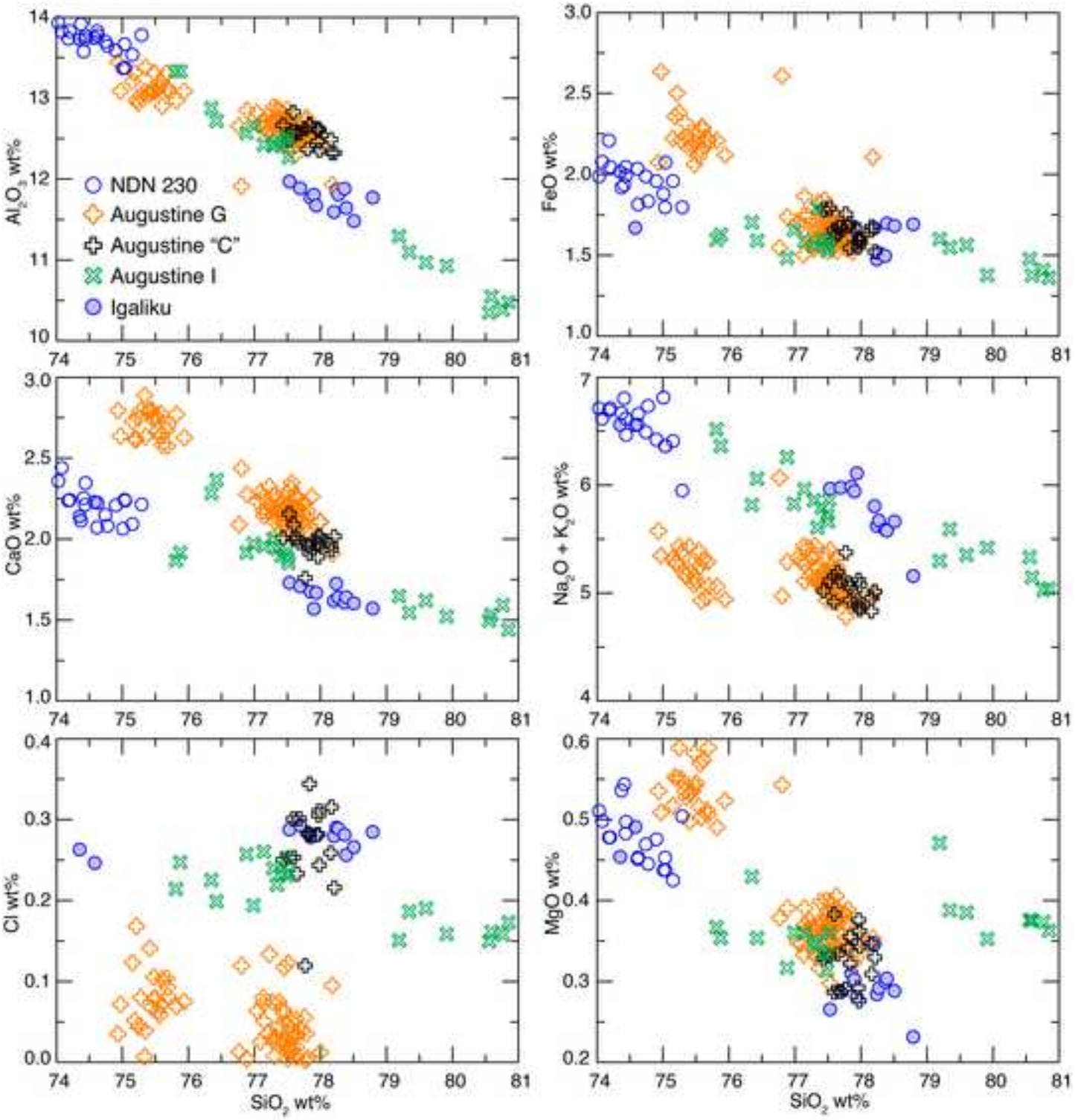

Figure 8

ACCEPTED MANUSCRIPT

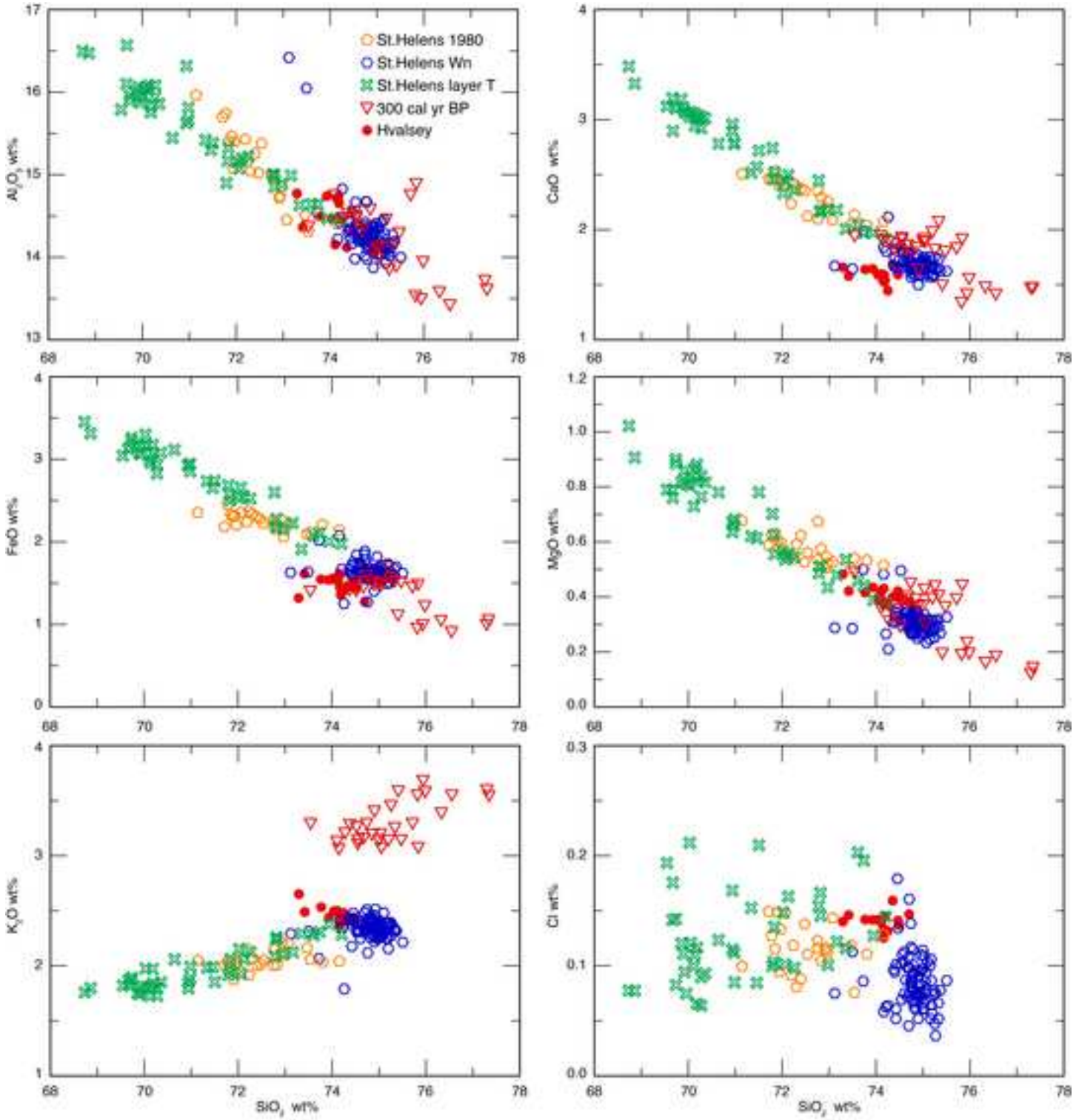

ACCEPTED MANUSCRIPT

Table 1 Radiocarbon dates from sites in the Eastern Settlement of Greenland. Post-bomb ^{14}C age estimates (marked *) show radiocarbon activity as a fraction of modern ($F^{14}C$). HA = humic acid.

Depth (cm)	Material	Lab code	^{14}C yr BP (±1σ)	cal AD (95.4% confidence)	$\delta^{13}C$ (‰)
Herjolfsnes					
17.0-16.0	Bulk peat (HA)	SUERC-24660	65±35	1689-1955	-26.7
21.0-20.0	Twig	SUERC-24664	*1.1169±0.0047	1957-1999	28.6
27.0-26.0	Charcoal fragments	SUERC-25010	825±55	1045-1280	–
35.0-34.0	Charcoal fragments	SUERC-24665	1020±35	902-1150	-24.8
35.0-34.0	*Montia fontana* seeds	SUERC-25012	975±100	780-1265	–
38.0-37.0	Charcoal fragments	SUERC-24666	1105±35	779-1018	-24.3
38.0-37.0	*Montia fontana* seeds	SUERC-24867	835±90	1019-1297	–
42.0-41.0	Charcoal fragments	SUERC-24667	960±35	1018-1158	-25.0
42.0-41.0	Bryophytes**	SUERC-24668	980±35	994-1154	-24.9
45.0-44.0	cf. *Betula* bark fragments	SUERC-24669	925±35	1025-1185	-30.8
45.0-44.0	Charcoal fragments	SUERC-24670	965±35	1016-1158	-25.3
Hvalsey					
7.0-6.0	*Sphagnum* section Acutipholia leaves	SUERC-19848	*1.0048±0.0040	1895 -1958	-23.8
10.0-9.0	*Sphagnum* section Acutipholia leaves	SUERC-19849	30±35	1694-1955	-24.0
11.0-10.0	Bulk peat (HA)	SUERC-4319	*1.0336±0.0045	1955 2009	-29.5
19.0-18.0	Charcoal	SUERC-19850	725±35	1224-1381	-24.0
21.0-20.0	Bulk peat (HA)	SUERC-4320	460±35	1408-1482	-28.8
25.0-24.0	Charcoal	SUERC-19851	740±35	1219-1296	-24.3
Igaliku					
24.0-23.0	Bulk peat (HA)	SUERC-8376	430±35	1418-1618	-29.5
41.0-40.0	Bulk peat (HA)	SUERC-8375	2230±35	*384-204 cal BC*	-29.1

**Bryophyte stems, branches and leaves (*Philonotis fontana*, *Calliergon* cf. *giganteum*, *Plagiomnium ellipticum*)

Table 2

ACCEPTED MANUSCRIPT

Tephra	SiO2	TiO2	Al2O3	FeO	MnO	MgO	CaO	Na2O	K2O	F	Cl	P2O5	SO2
HV10cm	75.0041	0.2265	14.9012	1.4654	0.1118	0.3873	1.6081	4.7417	2.4435	0.0274	0.1344	0.0645	0.0044
HV10cm	73.3415	0.2221	14.0949	1.5157	0.1125	0.4146	1.5679	4.58	2.4049	0.0424	0.1389	0.0436	0.0101
HV10cm	73.3844	0.2366	14.3363	1.5307	0.1036	0.3932	1.5766	4.8585	2.474	0.0166	0.1406	0.0544	0.0085
HV10cm	73.9126	0.2302	14.1104	1.261	0.097	0.3771	1.6351	4.6935	2.384	0.0311	0.1453	0.0581	0.0049
HV10cm	73.7306	0.2346	14.1603	1.4215	0.1015	0.3918	1.655	4.691	2.351	0.0288	0.1354	0.0652	0.0107
HV10cm	74.2128	0.2331	14.1744	1.5449	0.1062	0.4176	1.5988	5.1116	2.5029	0.0222	0.1395	0.0618	0.0154
HV10cm	73.1499	0.2274	14.2825	1.5954	0.1118	0.4245	1.5078	4.7988	2.3311	0.0108	0.1236	0.0634	0.0088
HV10cm	73.1741	0.2257	14.4544	1.3406	0.1069	0.3715	1.5206	4.7975	2.3814	0.0484	0.143	0.0536	0.0131
HV10cm	73.2844	0.2336	14.4003	1.5372	0.1078	0.4137	1.6288	4.9773	2.5159	0.0361	0.1411	0.0602	0.0094
HV10cm	73.808	0.2319	14.7167	1.5379	0.1125	0.4338	1.6416	4.6439	2.4343	0.0508	0.1415	0.0644	0.0143
HV10cm	74.6954	0.2326	14.5353	1.4083	0.1134	0.3733	1.4555	5.0616	2.4952	0.0257	0.1323	0.0655	0.0052
HV10cm	71.9725	0.2283	14.0811	1.5841	0.1089	0.4129	1.5493	5.3813	2.4401	0.0501	0.1432	0.0593	0.0205
HV10cm	72.7394	0.2277	14.6614	1.3101	0.1006	0.4794	1.6462	5.1922	2.6319	0.0449	0.1391	0.0561	0.014
HV10cm	70.7457	0.2376	13.435	1.387	0.0988	0.3804	1.6053	4.6813	2.2994	0.0476	0.1515	0.0629	0.0144
HV10cm	*75.0234*	*0.2399*	*14.5201*	*1.5583*	*0.1067*	*0.4275*	*1.5562*	*0.0883*	*0.6831*	*0.0557*	*0.1426*	*0.0664*	*0.0188*
IG35cm	76.0131	0.2232	13.424	0.8942	0.0493	0.2777	1.2688	4.5012	2.8012	0.0203	0.1129	0.0498	0.0176
IG35cm	76.1161	0.329	11.6452	1.6135	0.0755	0.281	1.6732	4.2206	1.6342	0.064	0.2869	0.0223	0.0098
IG35cm	75.3718	0.3196	11.2876	1.4994	0.0748	0.2714	1.6132	4.1582	1.7497	0.0655	0.2712	0.0196	0.0056
IG35cm	72.896	0.3107	13.407	1.4035	0.0398	0.3276	1.2691	4.6194	3.1433	0.0594	0.1269	0.038	0.0042
IG35cm	79.2559	0.3239	12.015	1.5133	0.0634	0.3034	1.626	3.8978	1.7547	0.0637	0.2844	0.0265	0.0082
IG35cm	78.514	0.3308	11.6382	1.6733	0.0652	0.3481	1.6248	4.1958	1.6315	0.0683	0.2806	0.0212	0.0038
IG35cm	77.4556	0.3248	11.9564	1.721	0.0712	0.2652	1.7281	4.2769	1.683	0.0944	0.2872	0.0274	0.0106
IG35cm	76.5893	0.3266	11.6072	1.6377	0.0735	0.2974	1.5437	4.2013	1.6404	0.0819	0.2763	0.0278	0.0134
IG35cm	73.5501	0.3016	13.5525	1.6466	0.094	0.484	2.198	4.2959	2.1672	0.027	0.2431	0.0496	0.0063
IG35cm	77.9308	0.3234	11.7809	1.6174	0.0734	0.3105	1.6763	4.2284	1.7623	0.0873	0.2784	0.0196	0.0125
IG35cm	75.6059	0.3011	13.9578	2.0495	0.1015	0.4615	2.1754	4.5961	2.0725	0.0242	0.2675	0.0482	0.0237
IG35cm	79.4592	0.3267	11.8707	1.7059	0.0657	0.2334	1.5848	3.5942	1.607	0.0763	0.2872	0.0214	0.0149
IG35cm	78.764	0.3293	11.6984	1.7044	0.0596	0.3052	1.6495	3.932	1.6709	0.0813	0.2574	0.0213	0.003
IG35cm	77.8671	0.3312	11.7477	1.5068	0.0633	0.2906	1.6302	3.6744	1.9682	0.0785	0.2871	0.0278	0.0103
IG35cm	77.4903	0.3153	11.7476	1.4606	0.063	0.2813	1.7081	3.9095	1.6592	0.0731	0.2875	0.0258	0.0207
IG35cm	75.7305	0.326	11.0744	1.622	0.0764	0.2781	1.5471	3.8542	1.6085	0.0717	0.2567	0.0177	-0.0038